

Lessons Learned from Study of Ice Clouds and Dust Aerosols Using MODIS and POLDER Observations

P. Yang, G. Hong, Z. Zhang, Q. Feng H.-M Cho and A. E. Dessler

Department of Atmospheric Sciences, Texas A&M University

Byan Baum

Space Science and Engineering Center/University of Wisconsin-Madison

Jerome Riedi

Laboratoire d'Optique Atmospherique, Universite de Lille, France

Outline

1. Study of the radiative forcing of ice clouds on the basis of collocated MODIS, AIRS and CERES data -- test a new parameterization of ice cloud radiative properties for climate models
2. Study of cloud phase based on MODIS and CALIPSO data
3. Effect of dust nonsphericity on the optical and radiative properties of dust aerosols -- application to the "deep blue" algorithm (Feng, Yang, Hsu, Tsay, and Laszlo)
4. Compare MODIS and POLDER retrievals of cirrus clouds

Part I

Study of the radiative forcing of ice clouds on the basis of collocated MODIS, AIRS and CERES data -- test a new parameterization of ice cloud radiative properties for climate models

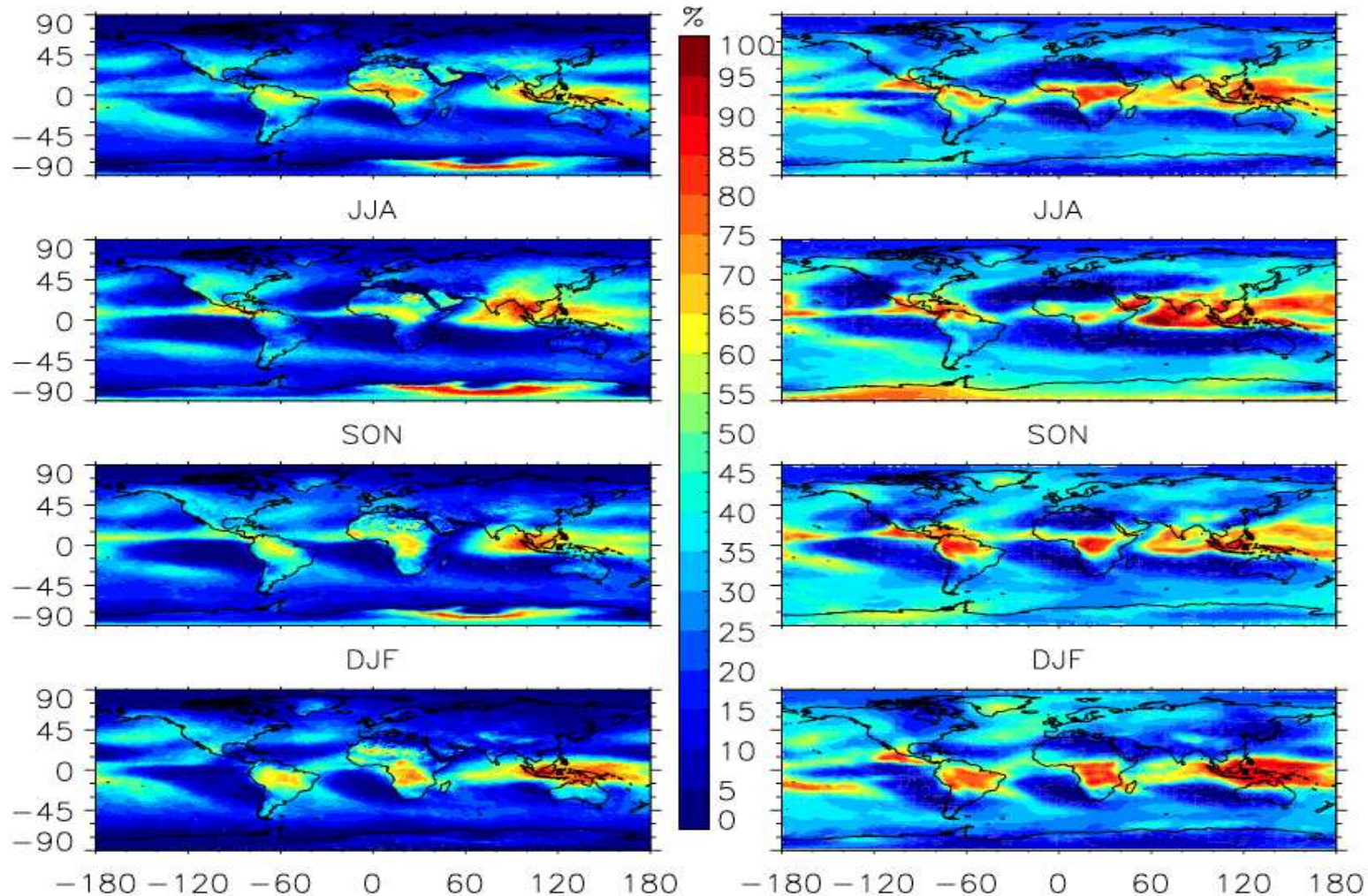
High Cloud Fraction (3-yr seasonal mean)

Terra(2000–2002)

MAM

CAM(1999–2001)

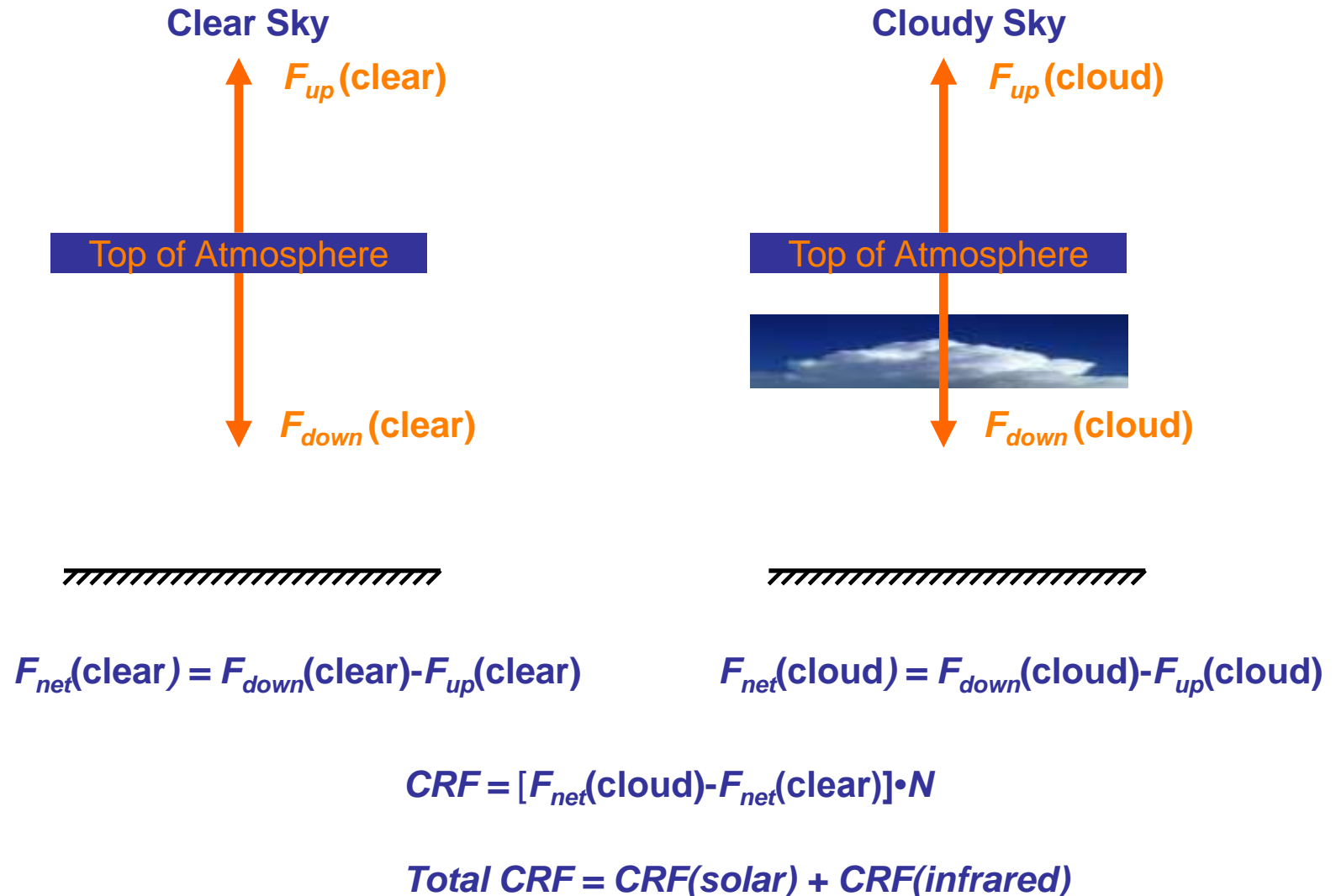
MAM



High cloud fraction 3-year average for Northern Hemisphere Spring (MAM), Summer(JJA), Fall(SON), and Winter(DJF).

Credit: Yue Li

Concept of Cloud Radiative Forcing

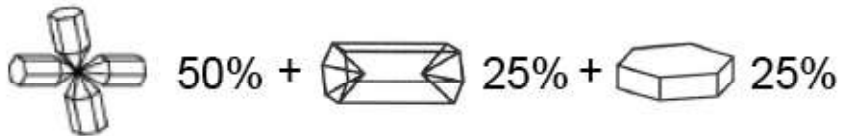


Ice cloud models: MODIS Collection 004 vs 005

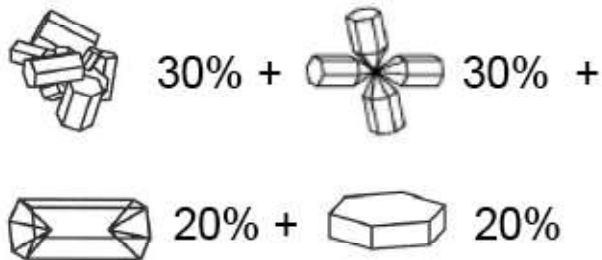
Mixing schemes for ice cloud particles

MODIS Collection 4 (King et al., 2004)

Particle's maximum dimension $D < 70 \mu\text{m}$



$70 \mu\text{m} < D$



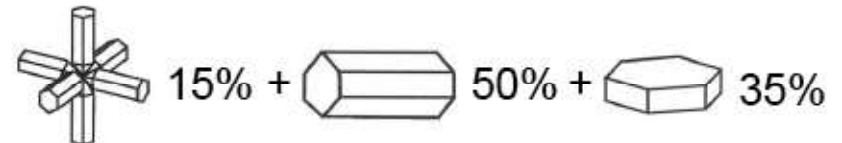
Mixing schemes for ice cloud particles

MODIS Collection 5 (Baum et al. 2005; King et al., 2007)

Particle's maximum dimension $D < 60 \mu\text{m}$



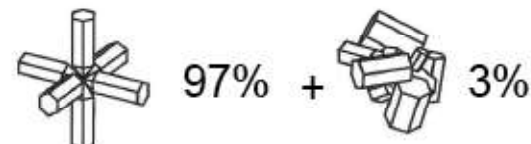
$60 \mu\text{m} < D < 1000 \mu\text{m}$



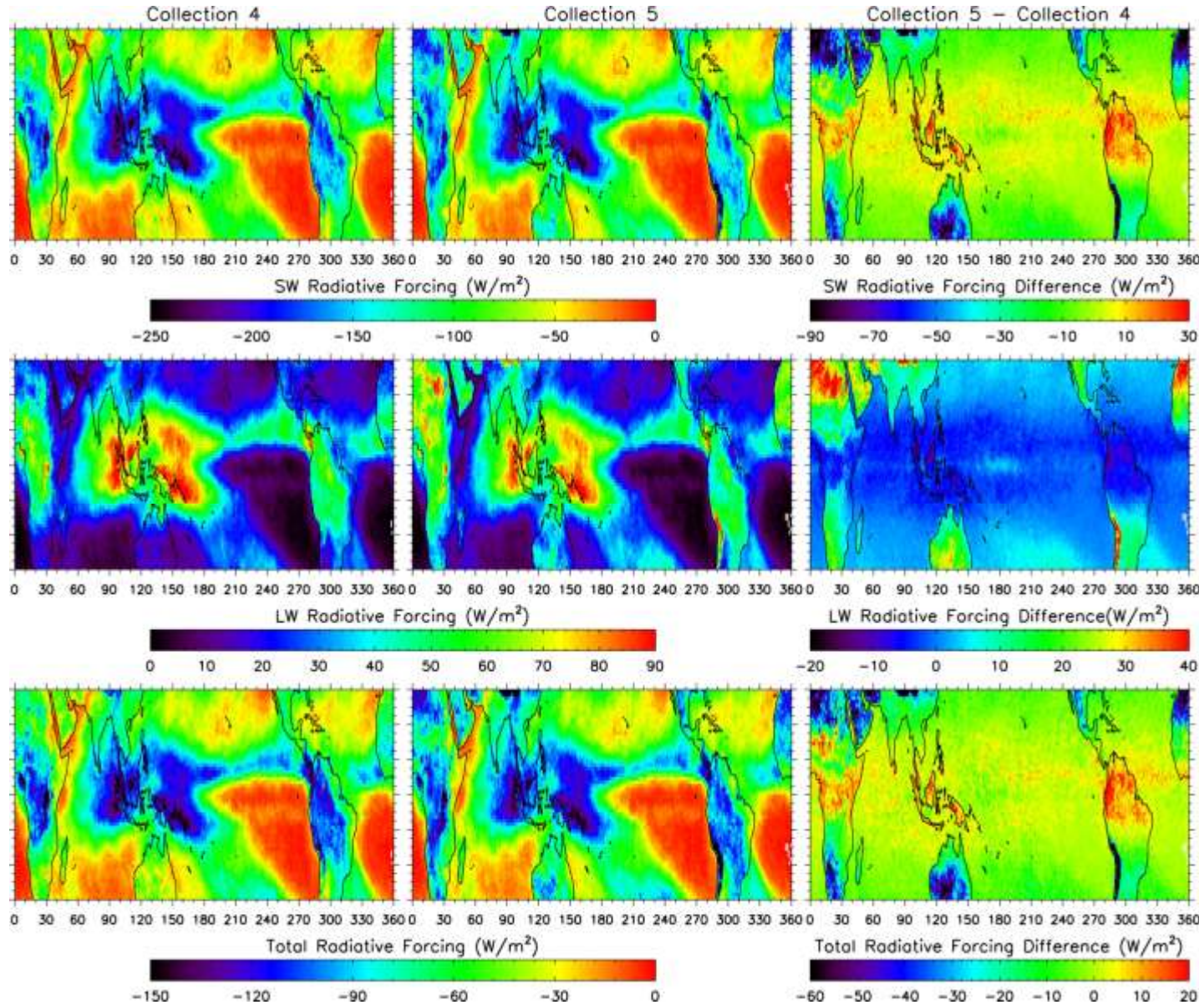
$1000 \mu\text{m} < D < 2500 \mu\text{m}$



$2500 \mu\text{m} < D$



Ice cloud Radiative Forcing: MODIS Collection 004 vs 005



Solar zenith angle $\theta_0 = 60^\circ$, Duration of sunlight is assumed to be 12 hours, Tropical standard atmospheric profile

A ice cloud microphysical model
(Baum et al., 2005a)

$$n(D) = N_0 D^\mu e^{-\lambda D}$$

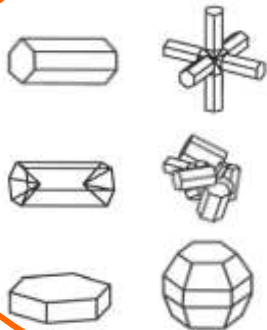
Field measurements from
TRMM, CRYSTAL-FACE
FIRE-I, -II, and ARM

For Retrieval

Narrow bands, e.g.
MODIS, SEVIRI,
GOES-R, (Baum et al.,
2005a,b)

High resolution
spectral bands, e.g.
AIRS, IASI, CrIS
(Baum et al., 2007)

For Climate Study

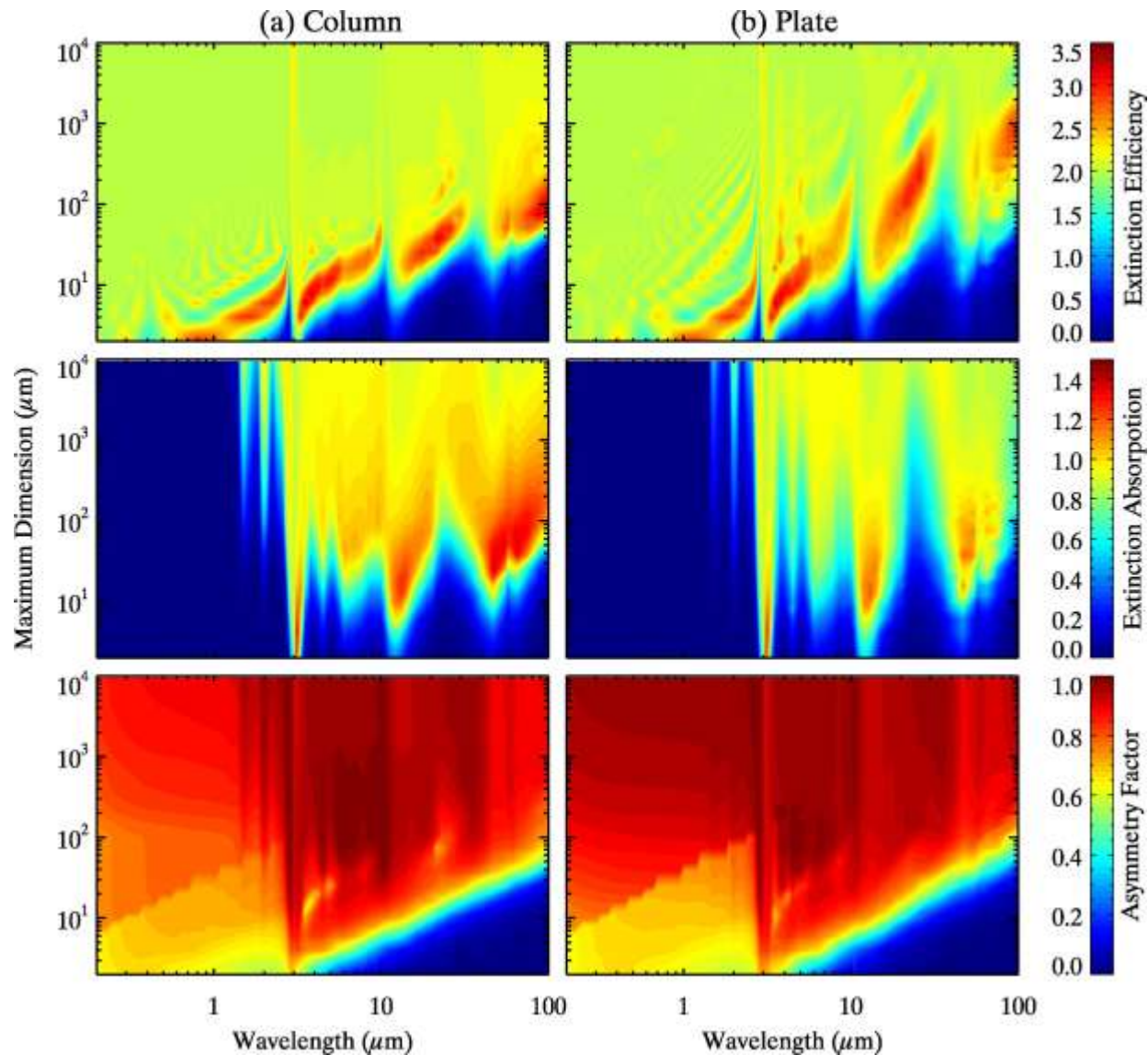


Single-scattering properties
(Yang et al, 2000, 2005)

- extinction efficiency
- single-scattering albedo
- asymmetry factor
- phase function

???

Modeling of the single-scattering properties of ice particles



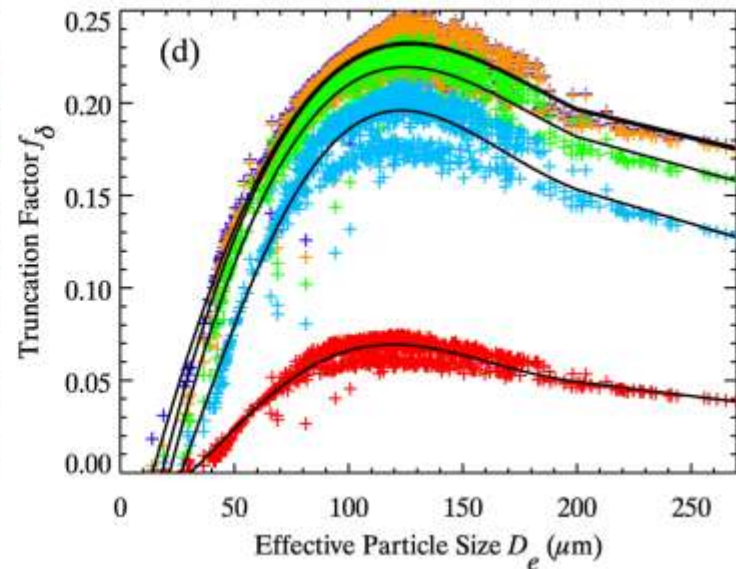
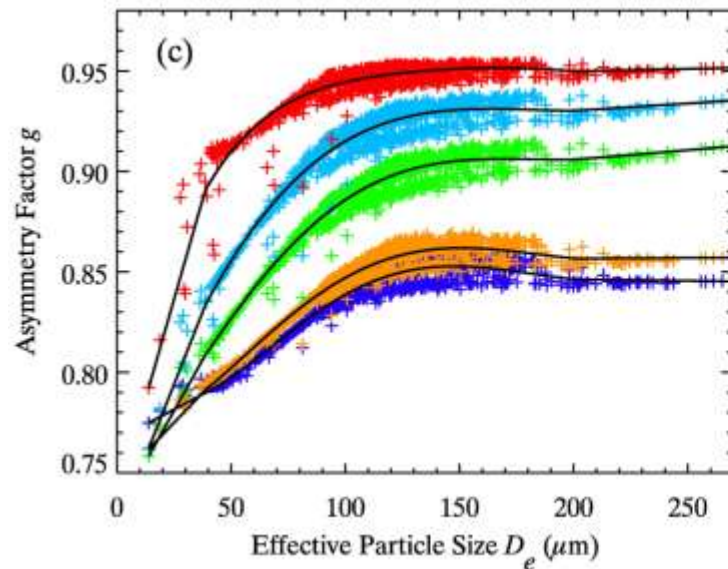
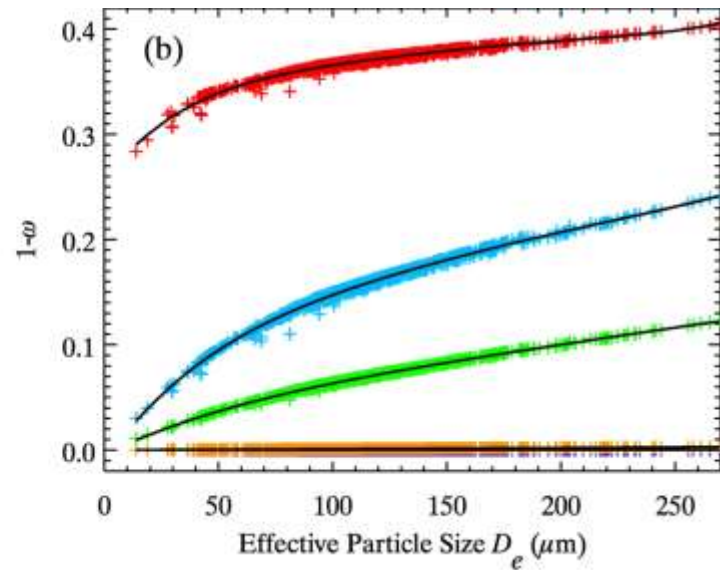
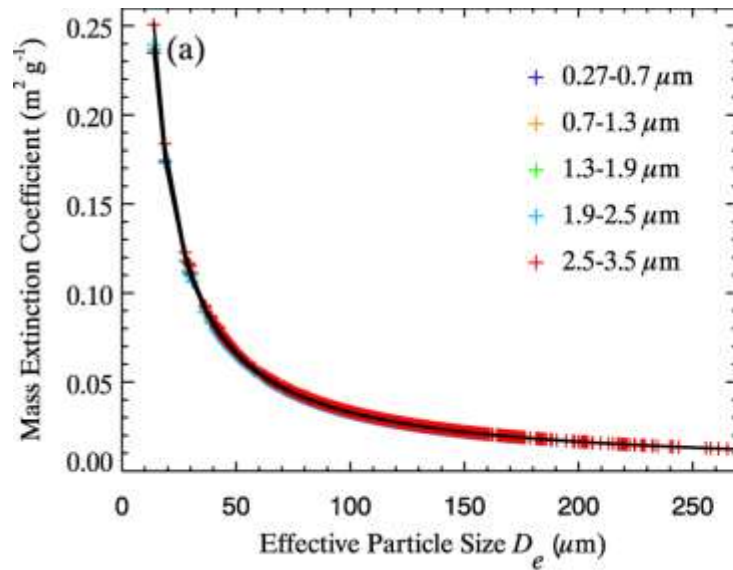
Particle Size Distribution

$$D_e = \frac{3 \int_{D_{\min}}^{D_{\max}} \left[\sum_{i=1}^N f_i(D) V_i(D) \right] N(D) dD}{2 \int_{D_{\min}}^{D_{\max}} \left[\sum_{i=1}^N f_i(D) A_i(D) \right] N(D) dD}$$

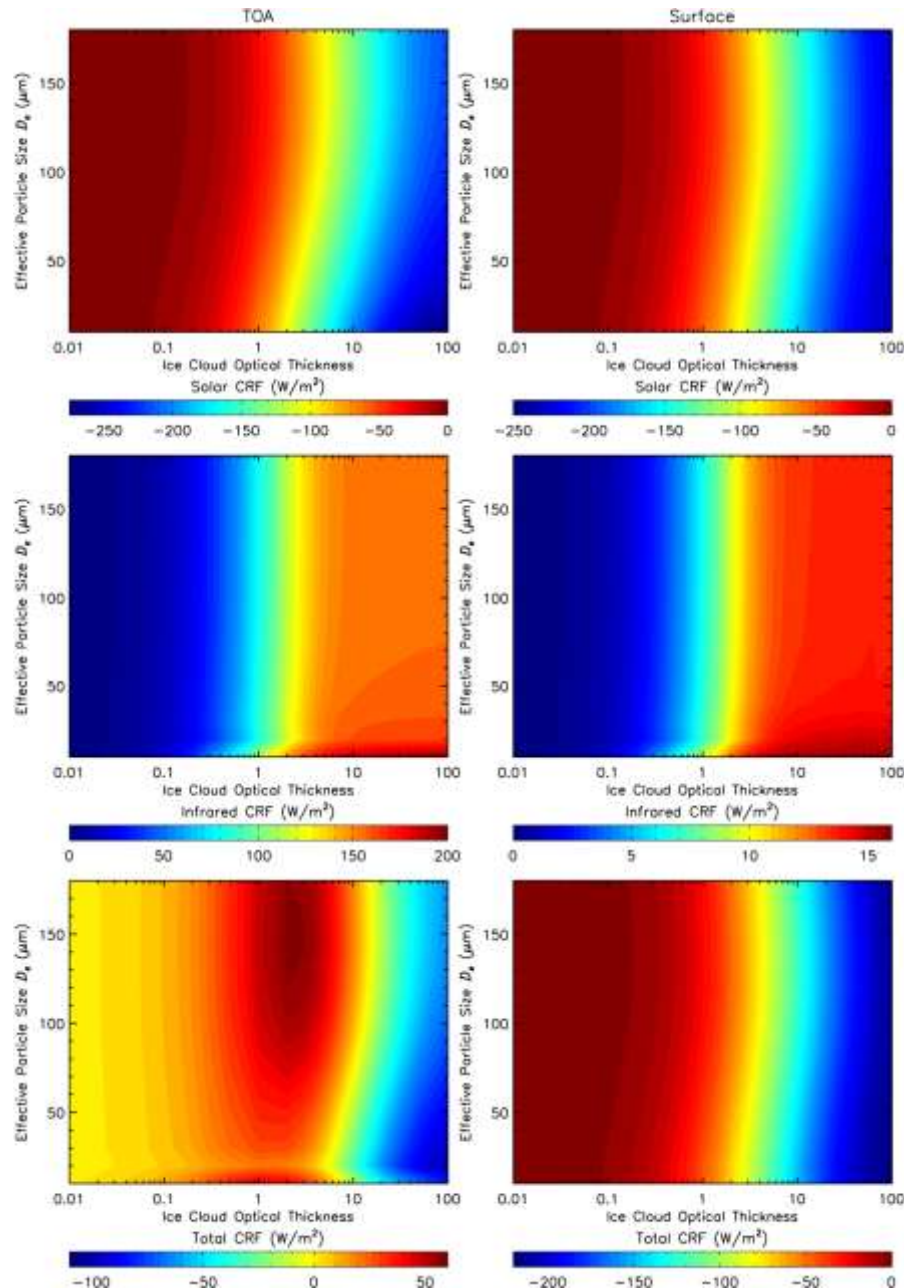
Field Campaign	Location and time	No. of total PSDs	No. of filtered PSD s
TRMM	Kwajalein, Marshall Islands, 1999	1133	418
CRYSTAL-FACE	Nicaragua/Caribbean, 2002	42	42
FIRE-I	Madison, WI, 1986	479	247
FIRE-II	Coffeyville, KS, 1991	23	22
ARM	Lamont, OK, 2000	390	390

Total 1140 PSDs (Heymsfield et al. 2003; Baum et al. 2005a)

Parameterization of Solar Scattering Properties



Ice Cloud Radiative Forcing



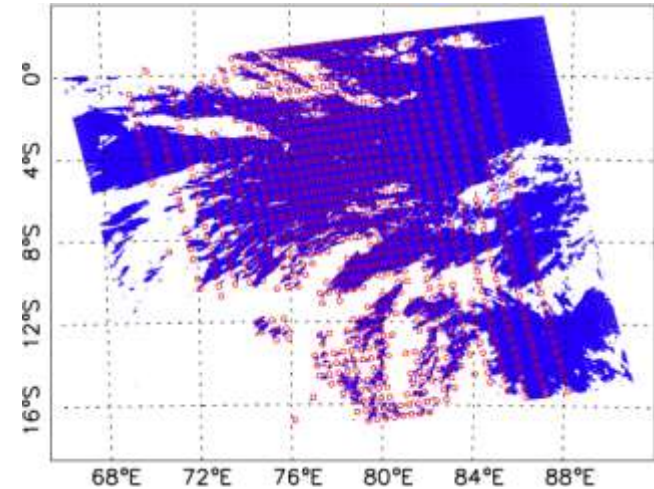
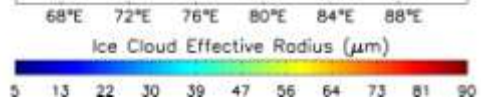
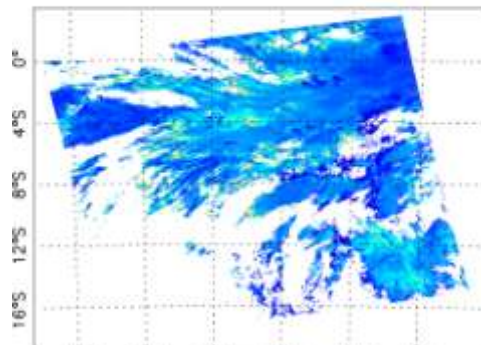
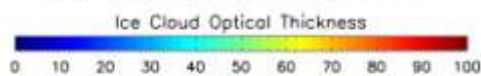
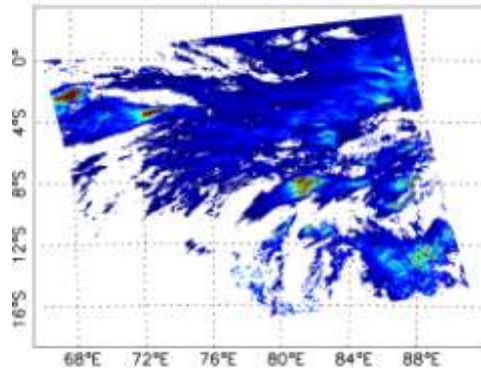
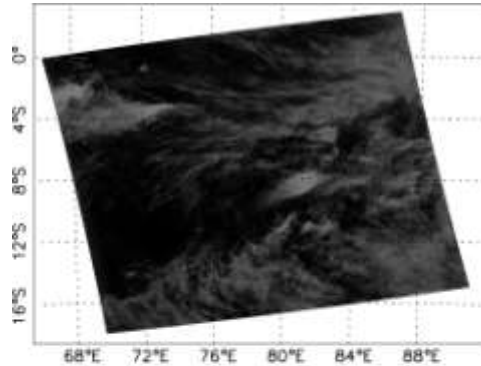
Cloud top height
 $H = 12 \text{ km}$

Geometrical thickness
 $\Delta Z = 1 \text{ km}$

Solar zenith angle
 $\theta_0 = 60^\circ$

Duration of sunlight is
assumed to be 12 hours

Ice Cloud Radiative Forcing



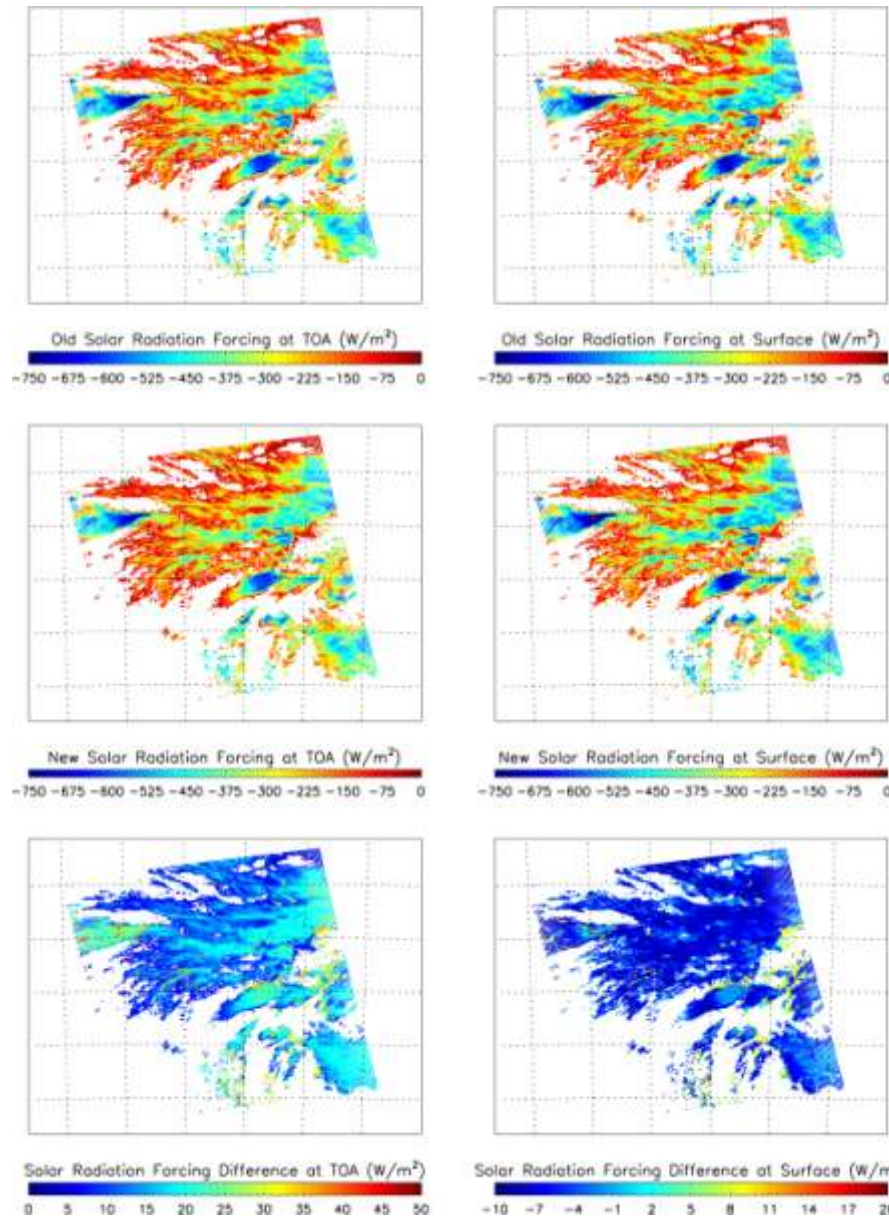
Collocated AIRS
Retrieved Atmospheric
Profiles

MODIS Retrieved
Ice Cloud Properties

RT model } New Param.

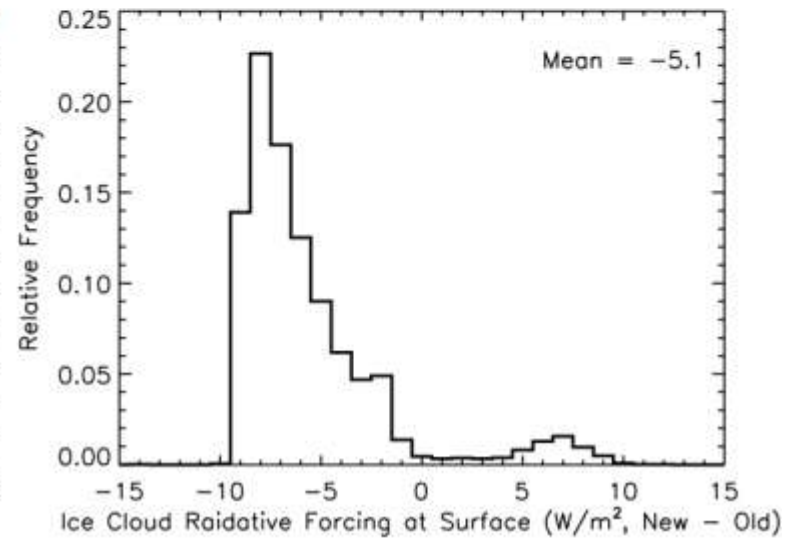
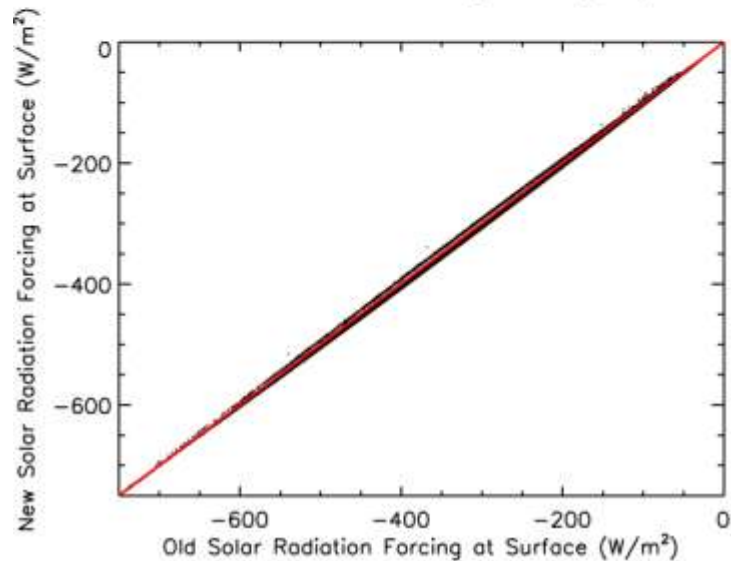
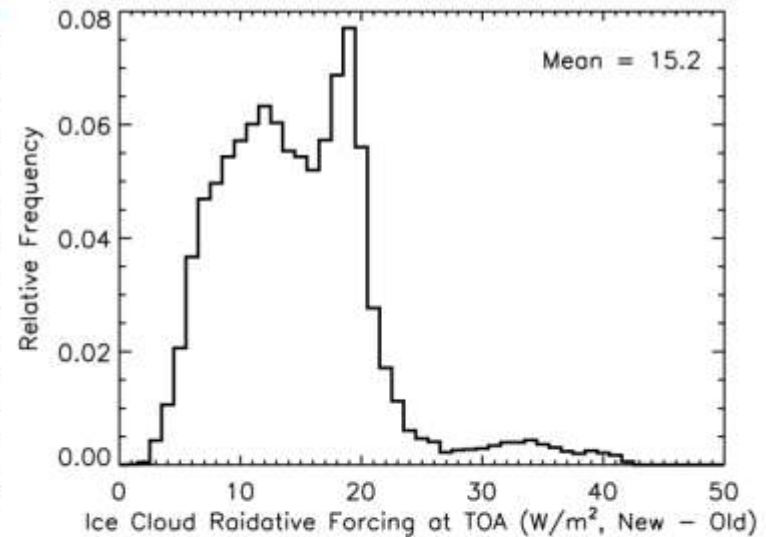
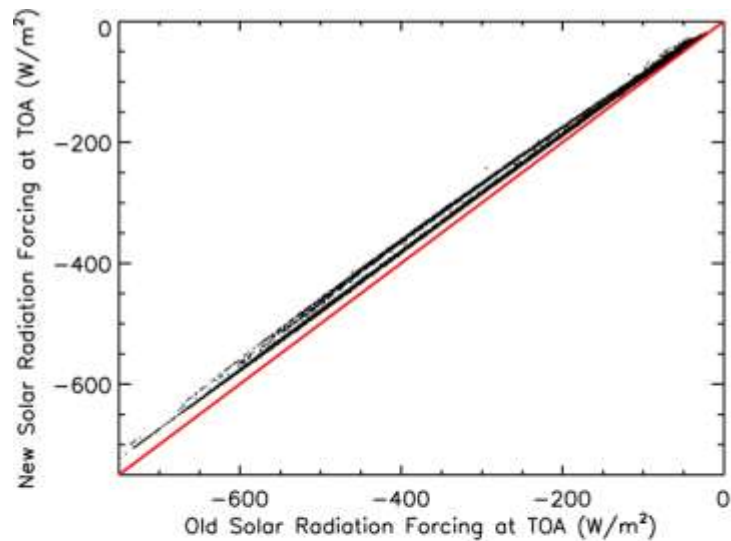
Ice Cloud Forcing

Ice Cloud Radiative Forcing: Solar

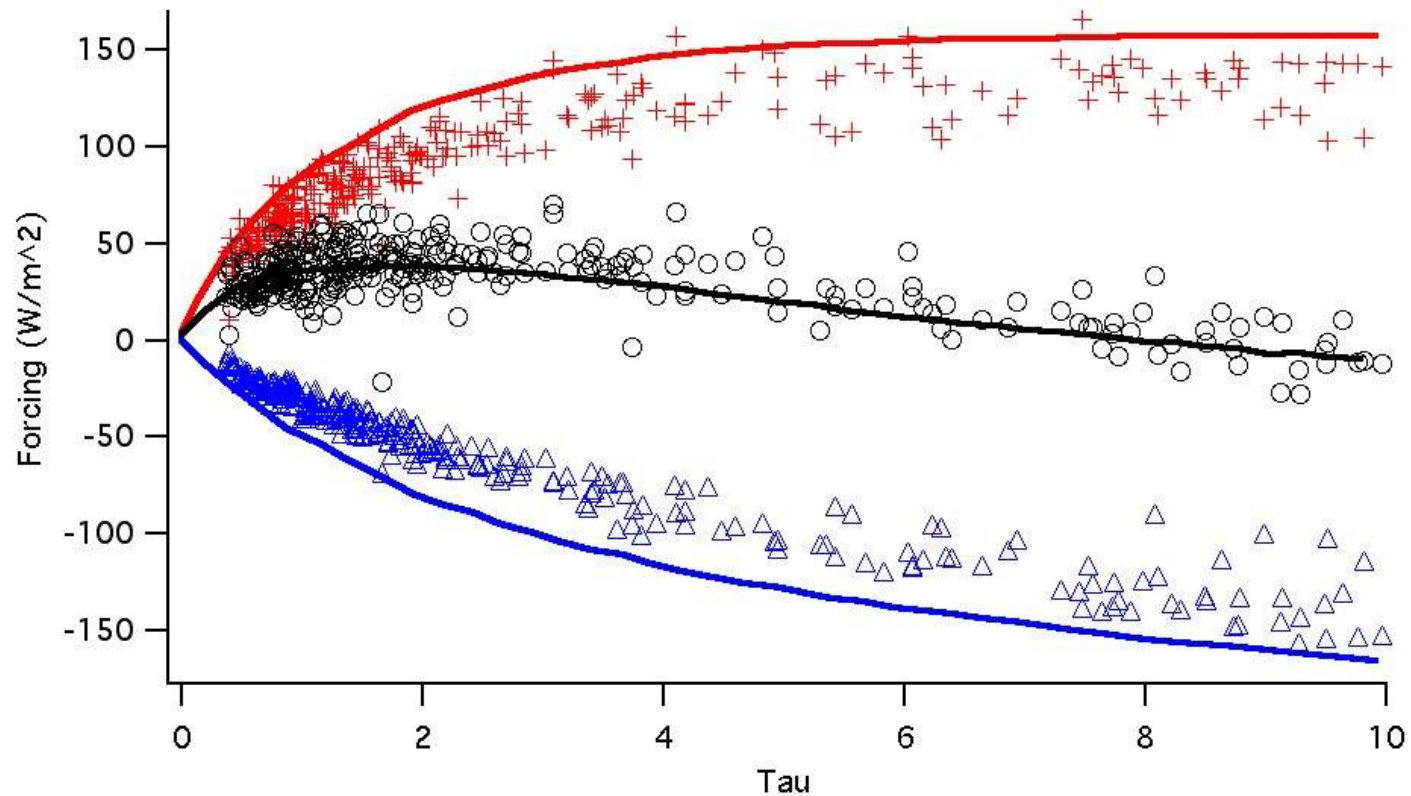


**Solar Radiative Forcing
With the
New Parameterizations**

Ice Cloud Radiative Forcing: Solar



Comparison of CERES Measurements (symbols) and Simulations (solid lines)



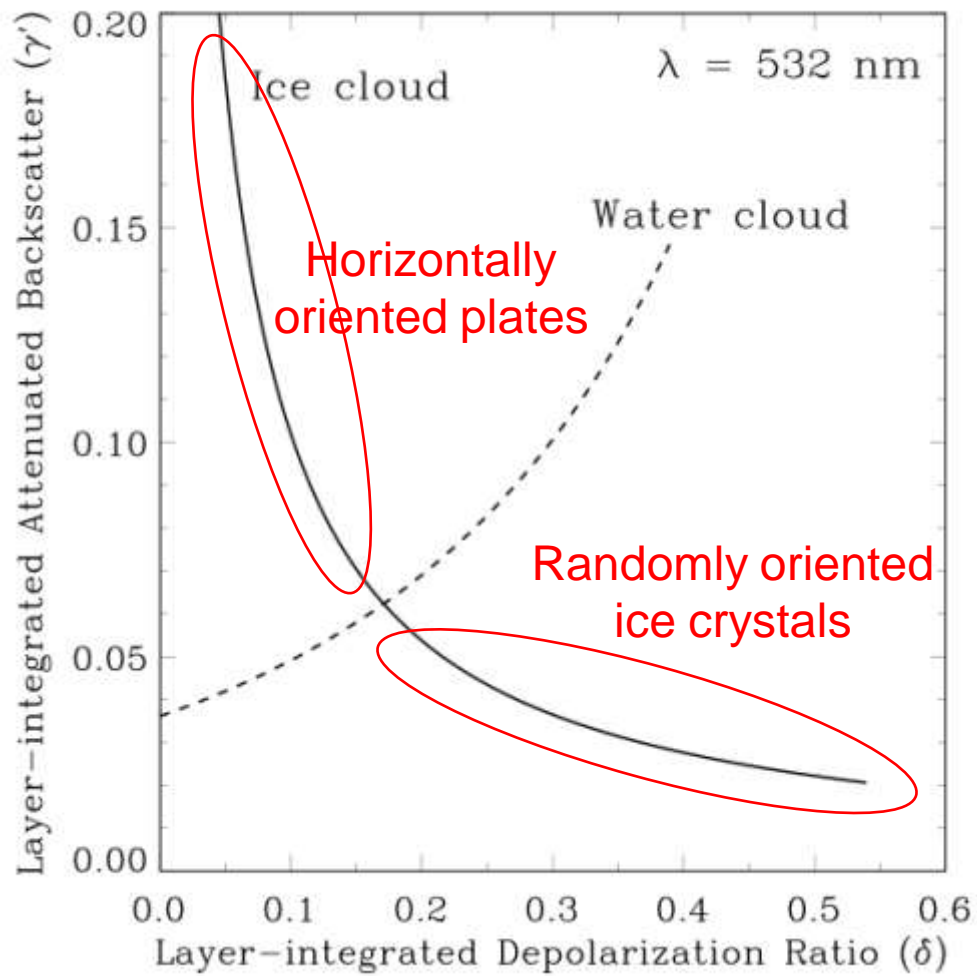
Data credit: A. E. Dessler and G. Hong

Part II

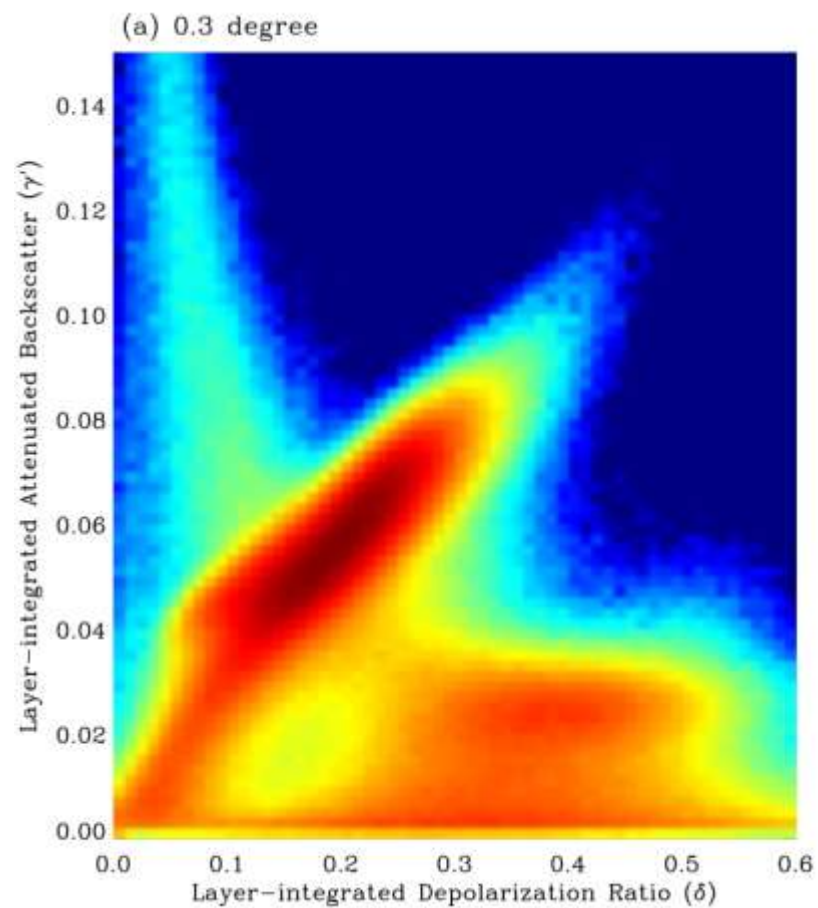
Study of cloud phase based on MODIS and CLIPSO data

Cho, H.-M., P. Yang, G. W. Kattawar, S. L. Nasiri, Y. Hu, P. Minnis, C. Trepte, and D. Winker, 2008: Depolarization ratio and attenuated backscatter for nine cloud types: analyses based on collocated CLIPSO lidar and MODIS measurements, *Optics Express*, 16, 3931-3948.

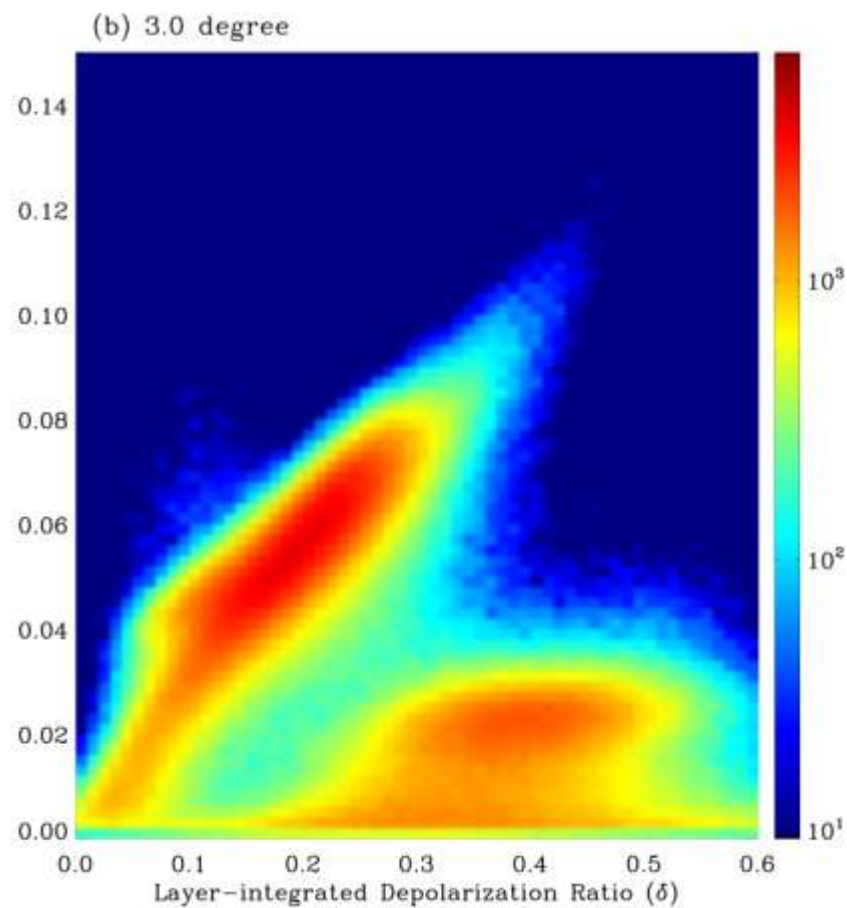
Hu, Y., M. Vaughan, Z. Liu, B. Lin, P. Yang, D. Flittner, B. Hunt, R. Kuehn, J. Huang, D. Wu, S. Rodier, K. Powell, C. Trepte, and D. Winker, 2007, the depolarization-attenuated backscatter relation: CLIPSO lidar measurements vs theory, *Optics Express* 15, 5327-5332.



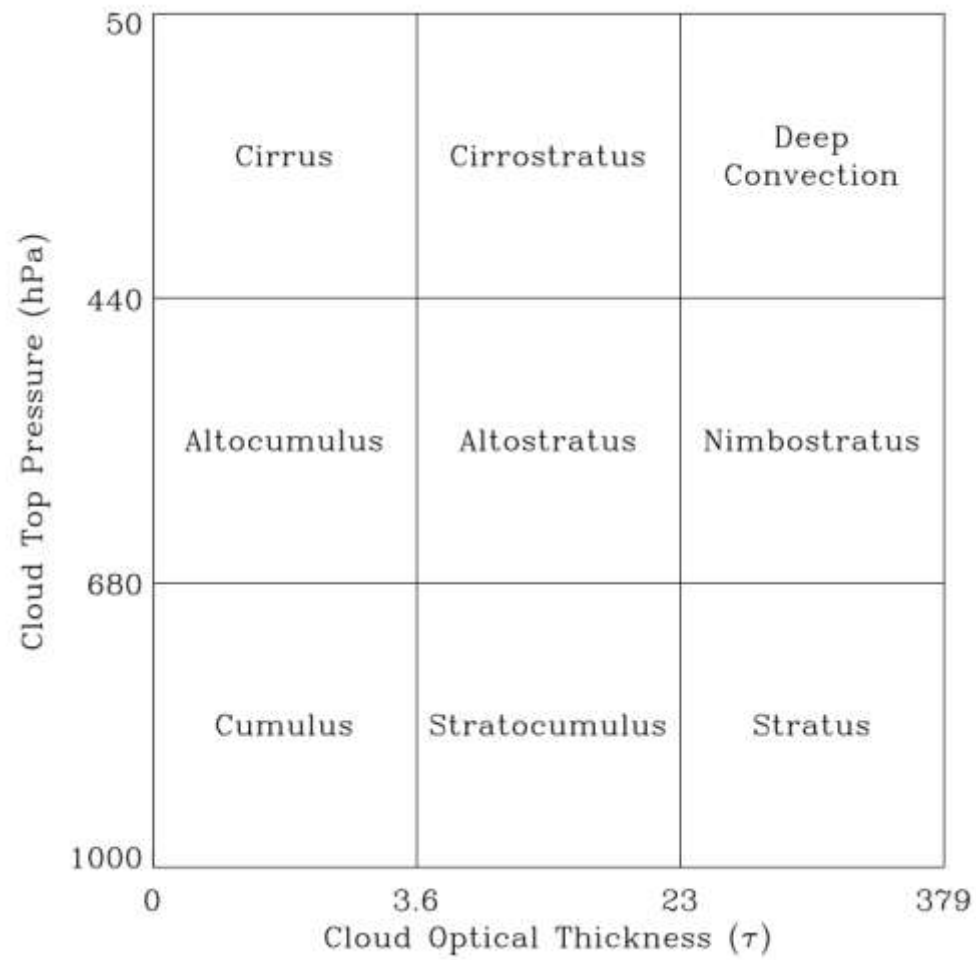
Hu et al.(2007)



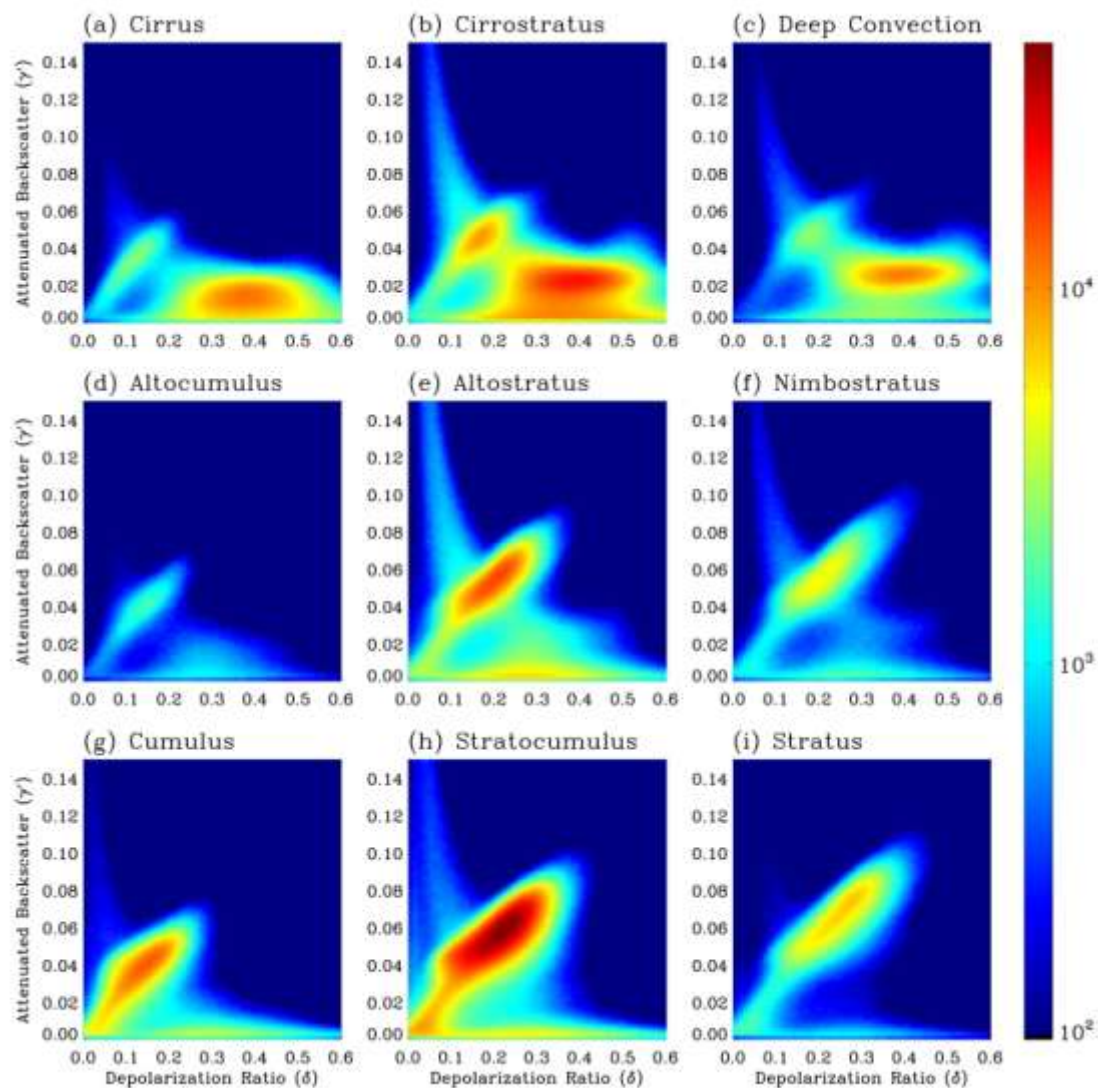
Aug. 1 - Aug. 21, 2007



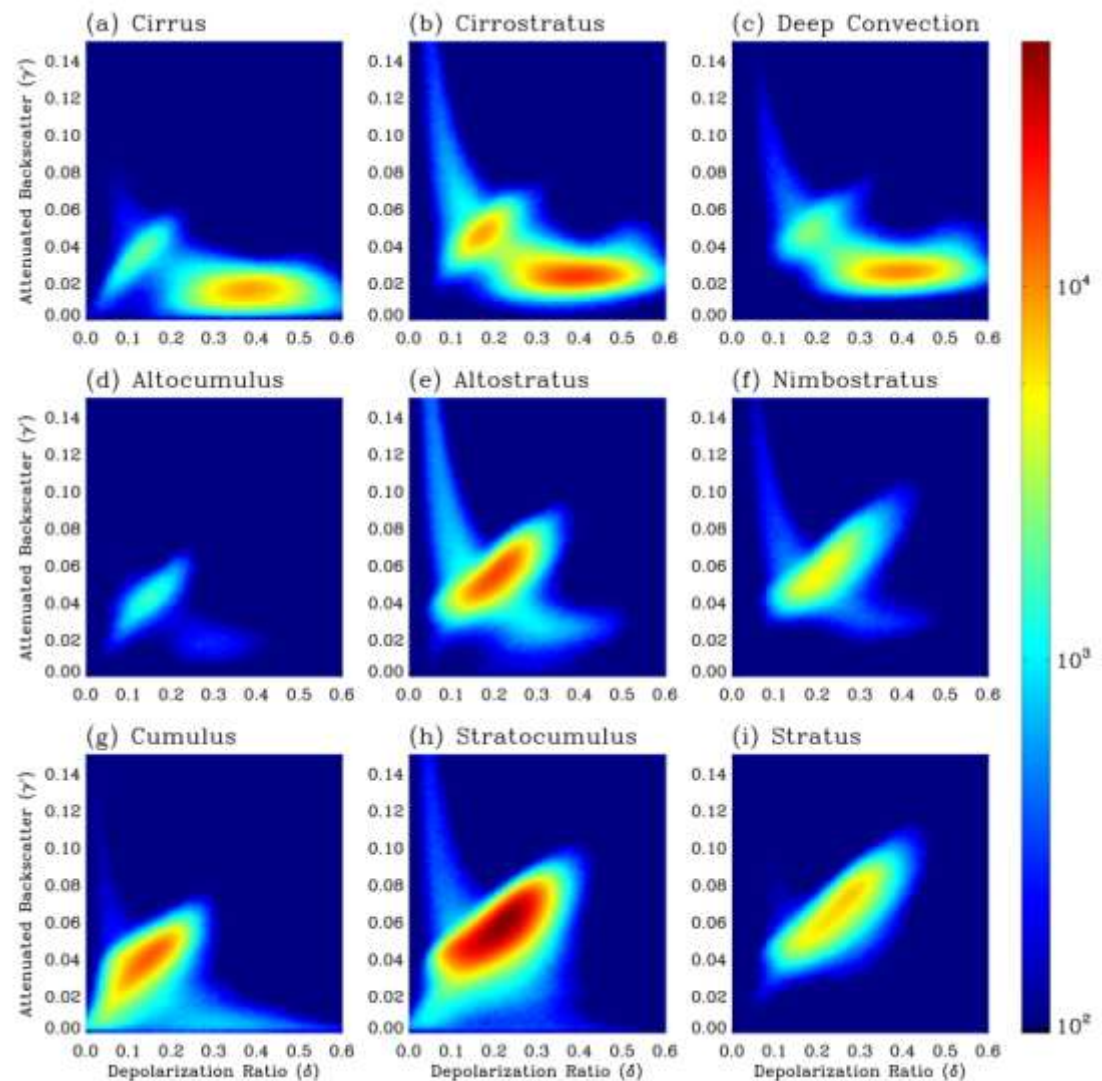
Aug. 21 - Aug. 31, 2007



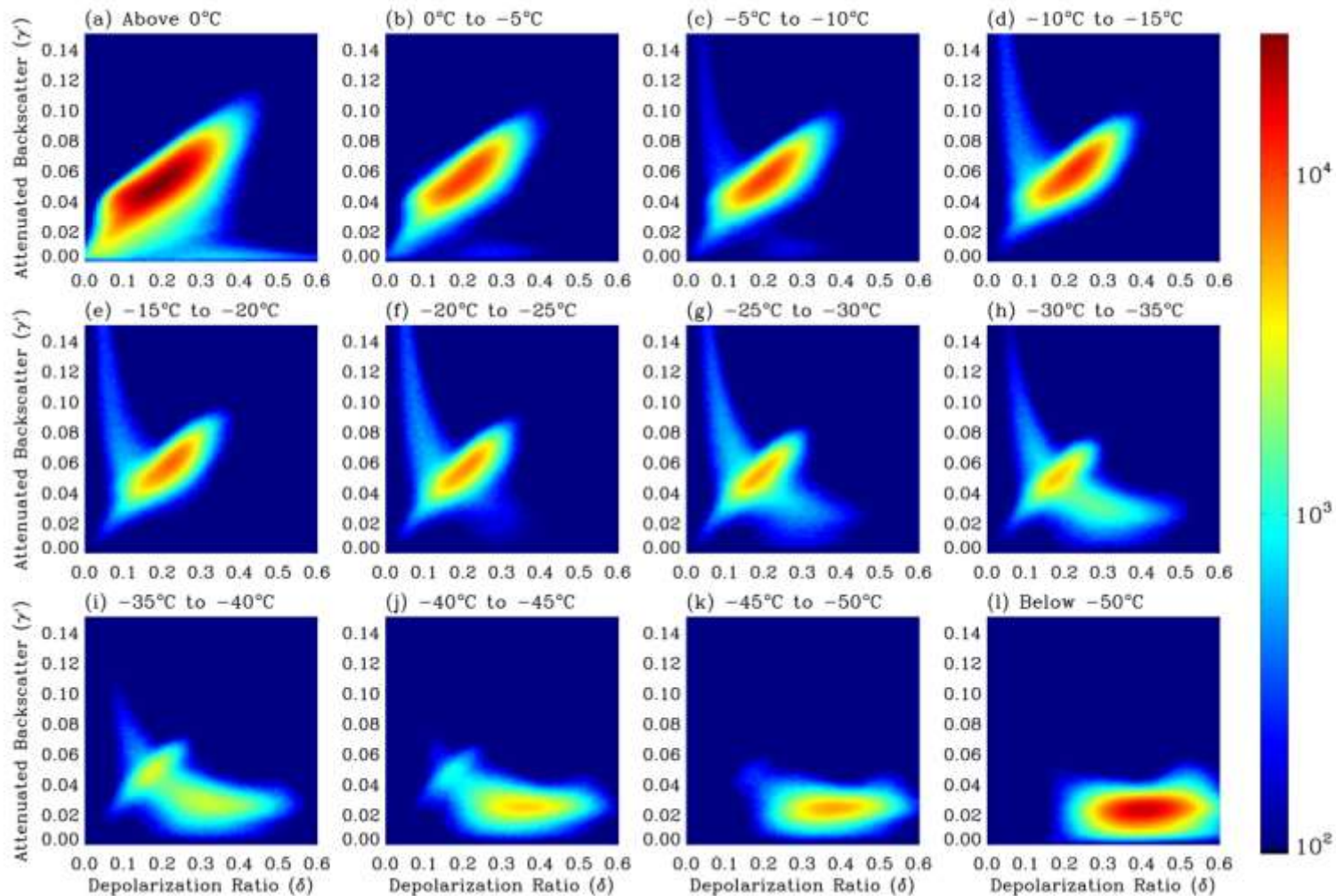
Top-most layer,
July, 2006 - June, 2007



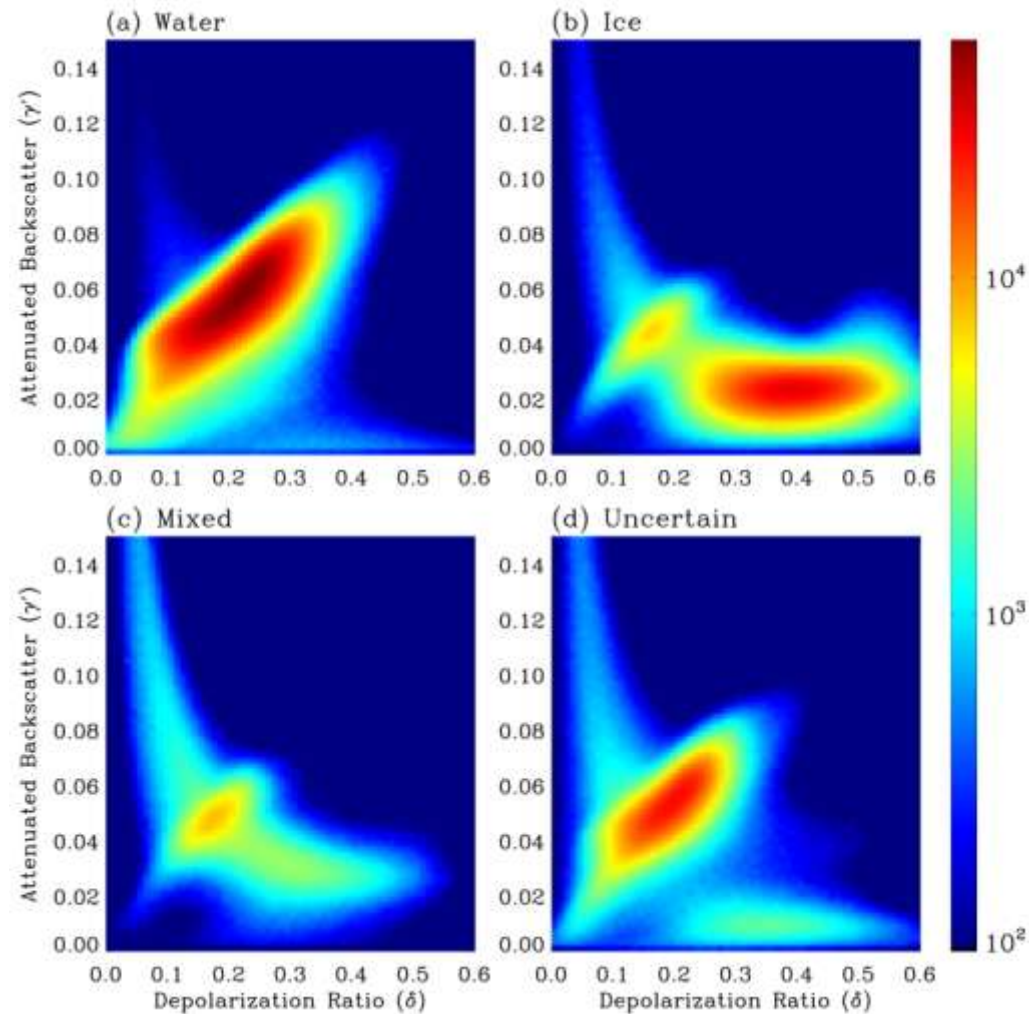
Single layer,
July, 2006 - June, 2007



Cloud phase vs. cloud-top pressure



Classification based on the MODIS cloud phase (bispectral IR algorithm)



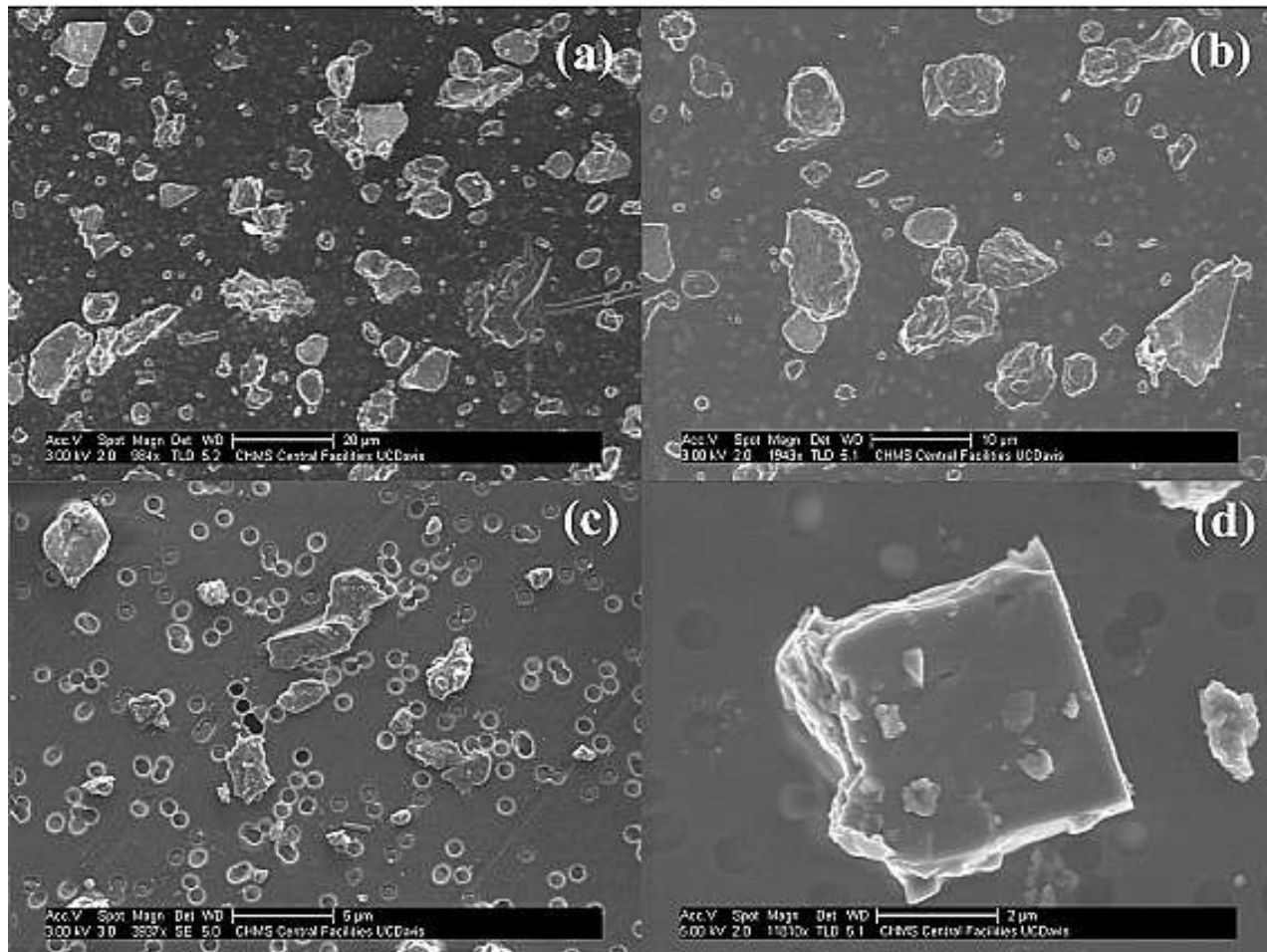
Part III

Effect of dust nonsphericity on the optical and radiative properties of dust aerosols -- application to the “deep blue” algorithm

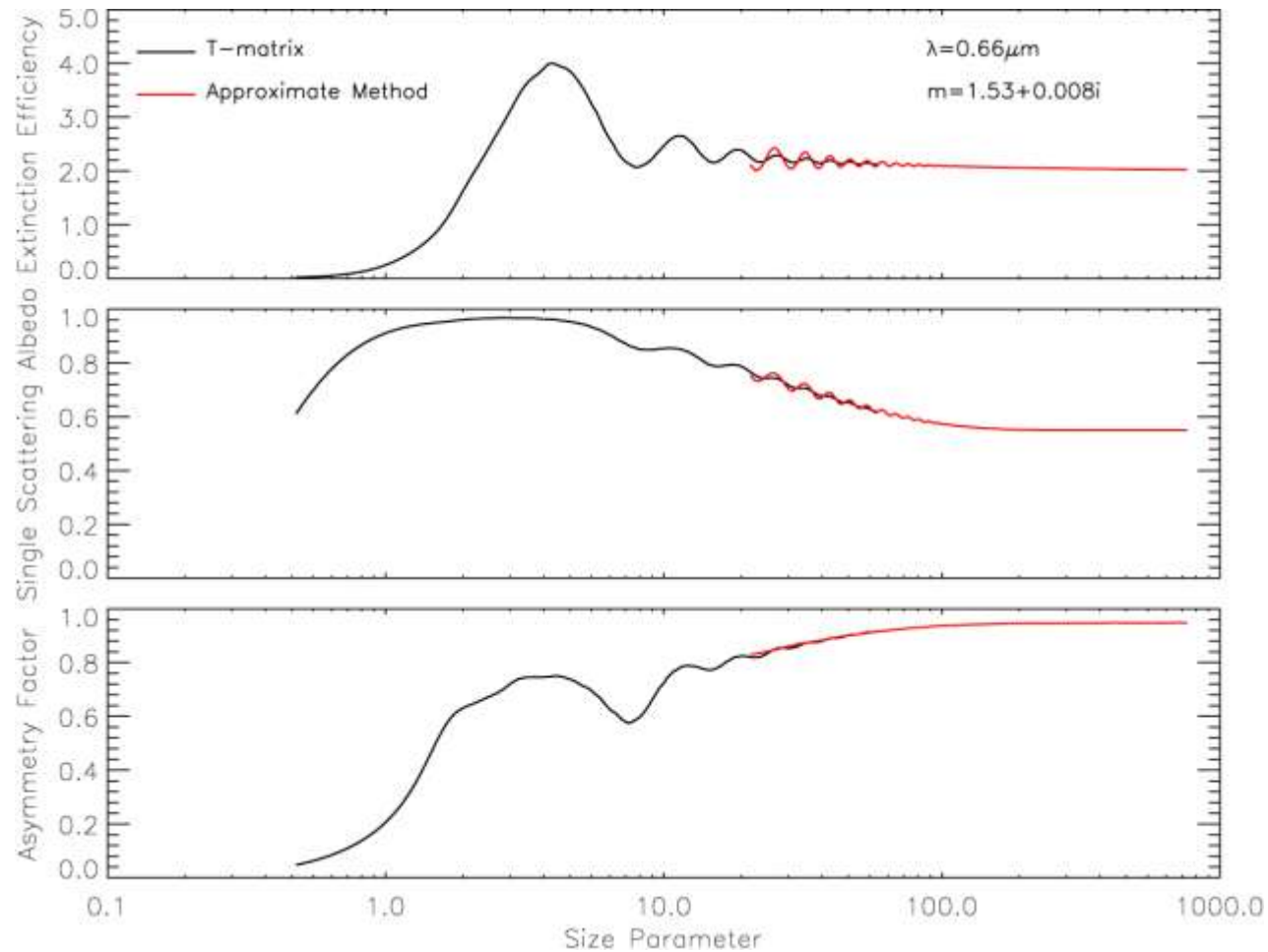
Qian Feng, Ping Yang, George Kattawar
Texas A&M University, College Station, TX

Christina N. Hsu and Si-chee Tsay
NASA Goddard Space Flight Center

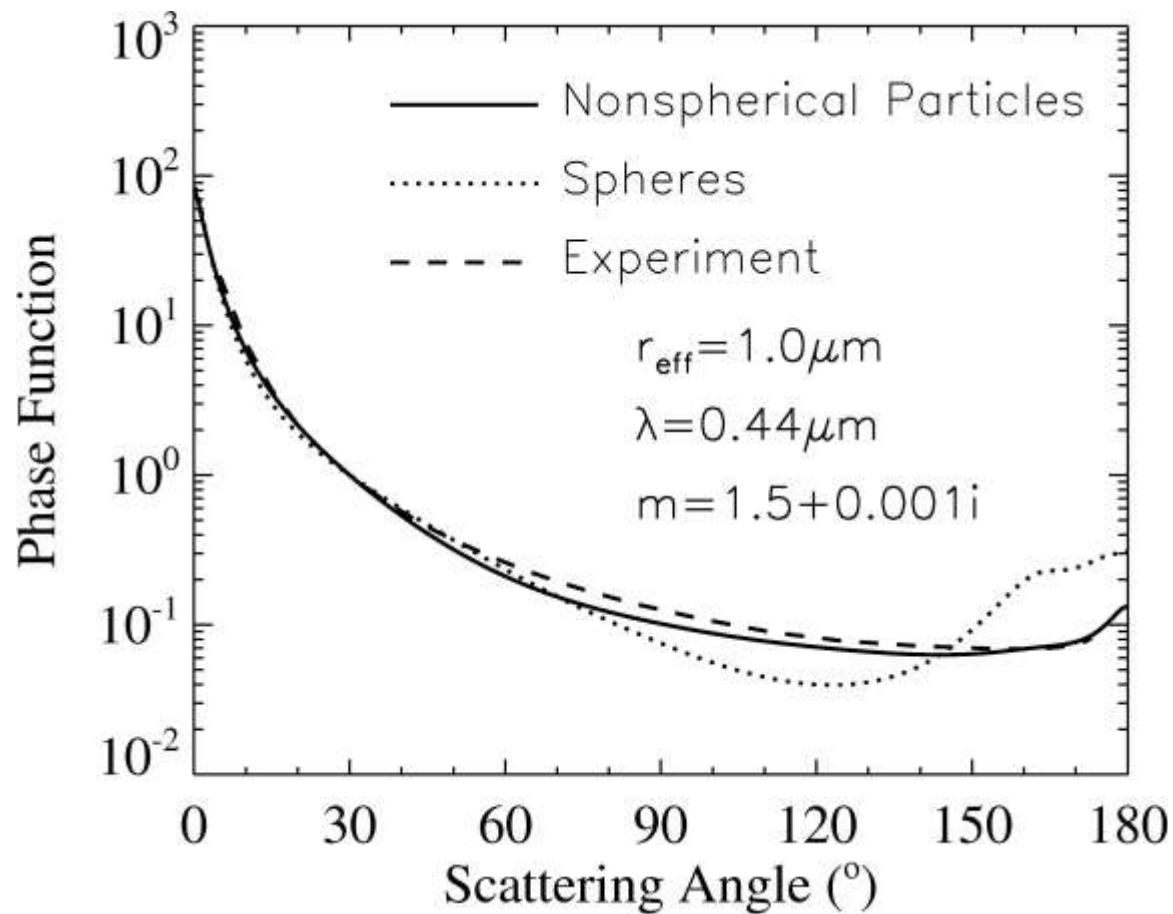
Istvan Laszlo
NOAA/NESDIS, Office of Research and Applications, Camp Spring,
MD 20746, USA



Secondary electron microscope images of dust particles collected in the Saharan Air Layer near Puerto Rico on 21 July 2000. Because some size segregation occurs on the filter substrate, size and shape distributions from individual images are not representative of the dust as a whole. (a) 1000X, (c) 2000X, (b) 4000X, and (d) 12000X. *The figure and figure caption are adapted from Reid et al. (2003).*

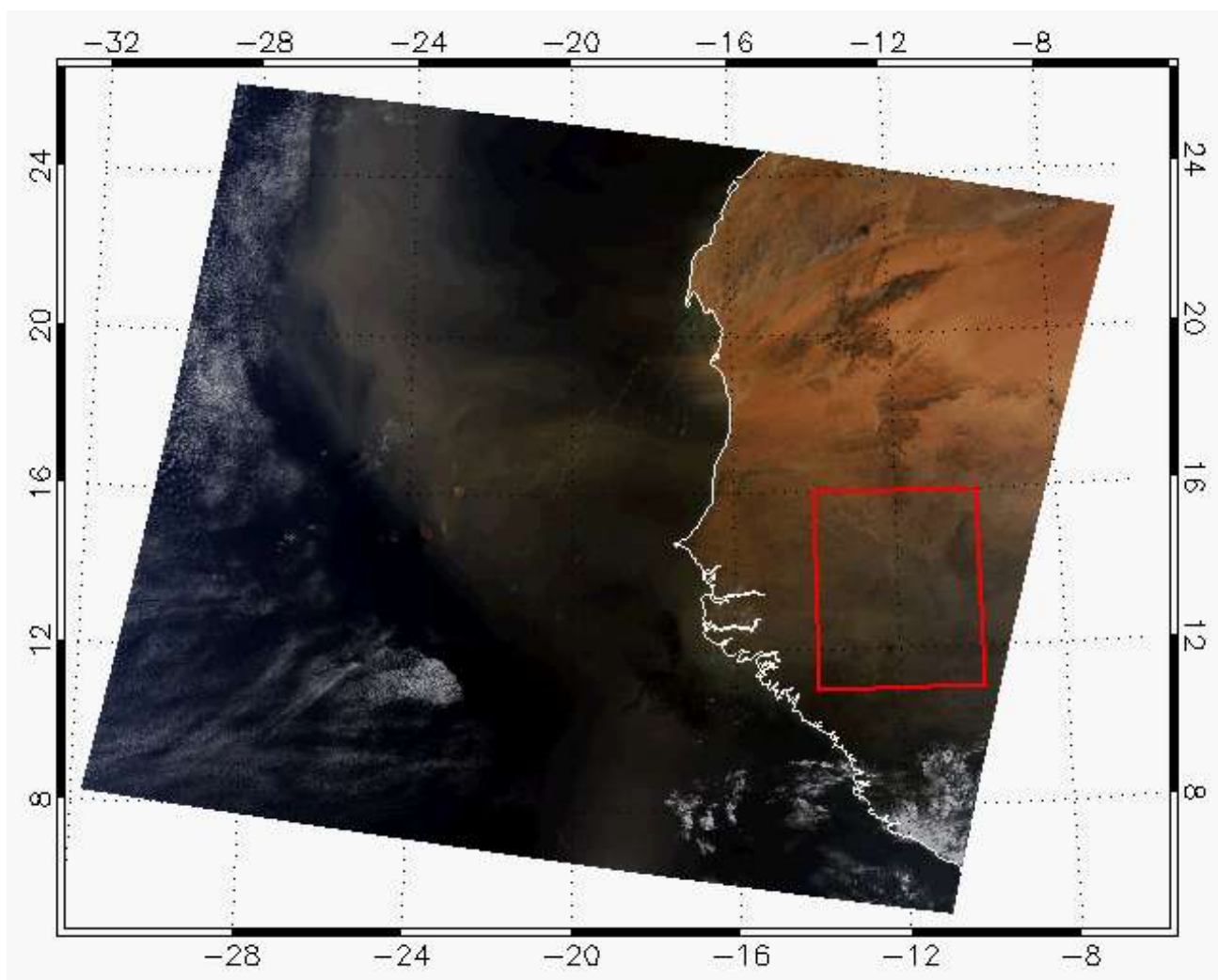


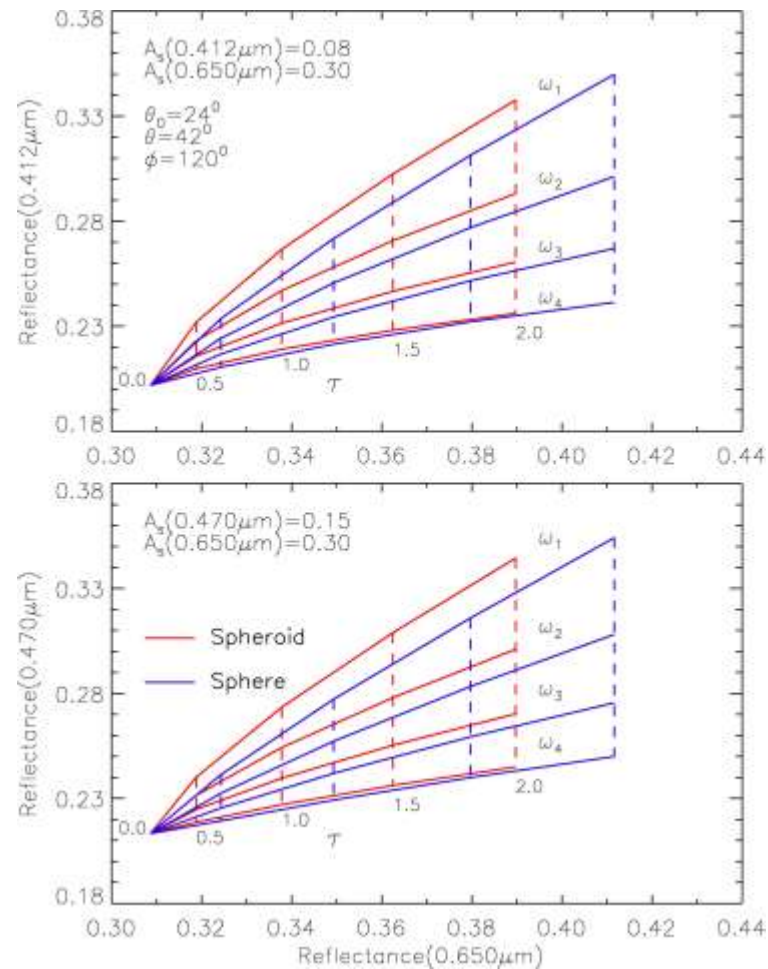
Comparison between the T-matrix (Mishchenko and Trvais, 1994) solutions and their counterparts computed from an approximate approach (Yang et al. 2007) for the optical properties of dust particles. The particle shape is assumed to be a prolate spheroid with an aspect ratio of 1.7. The size parameter indicated in the x-axis is defined in terms of that for the equivalent-volume sphere. Adapted from Yang et al. (2007).



Experimental data (Volten et al. 2005)

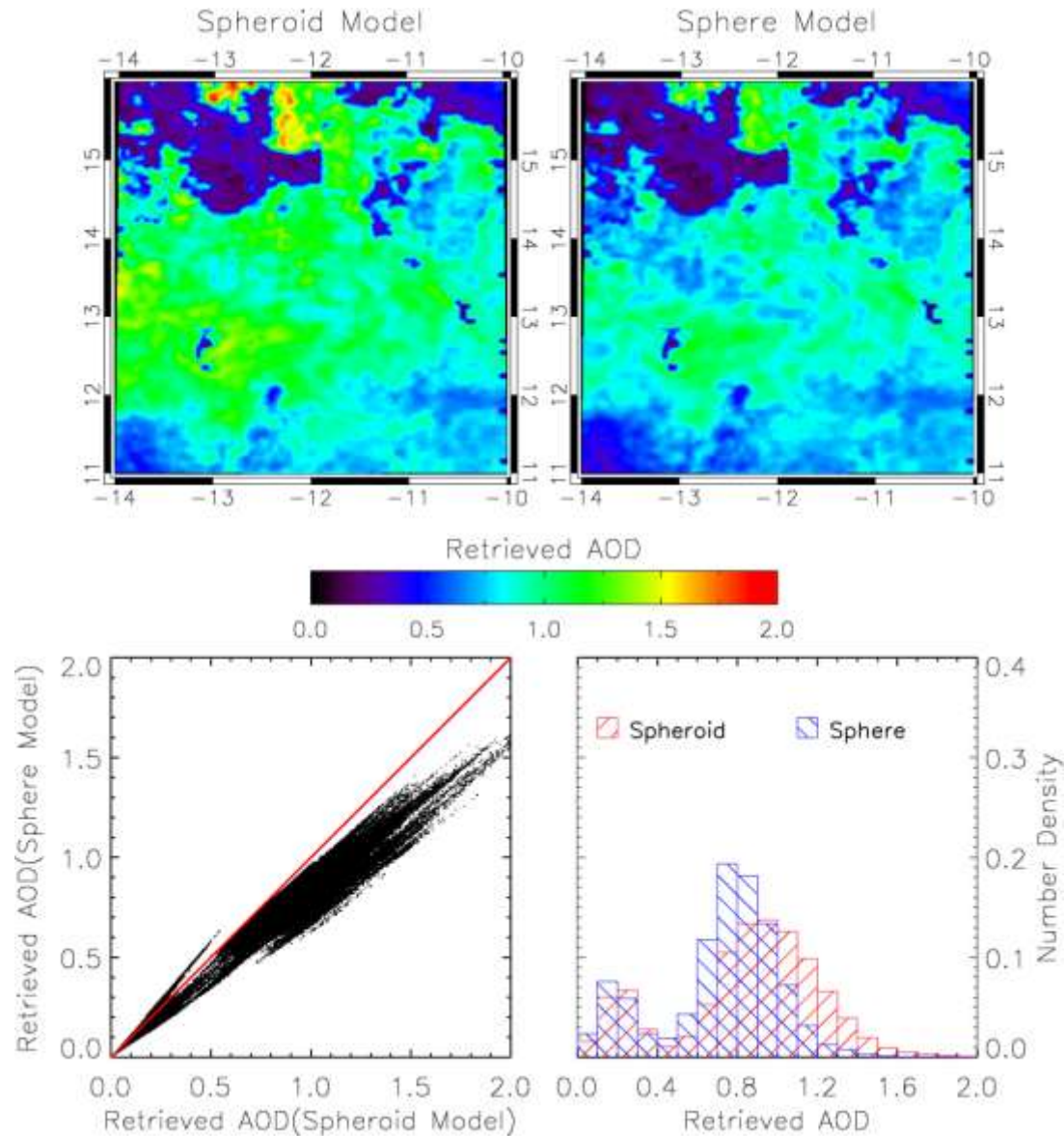
Theoretical simulation was based on the method of Yang et al. (2007)

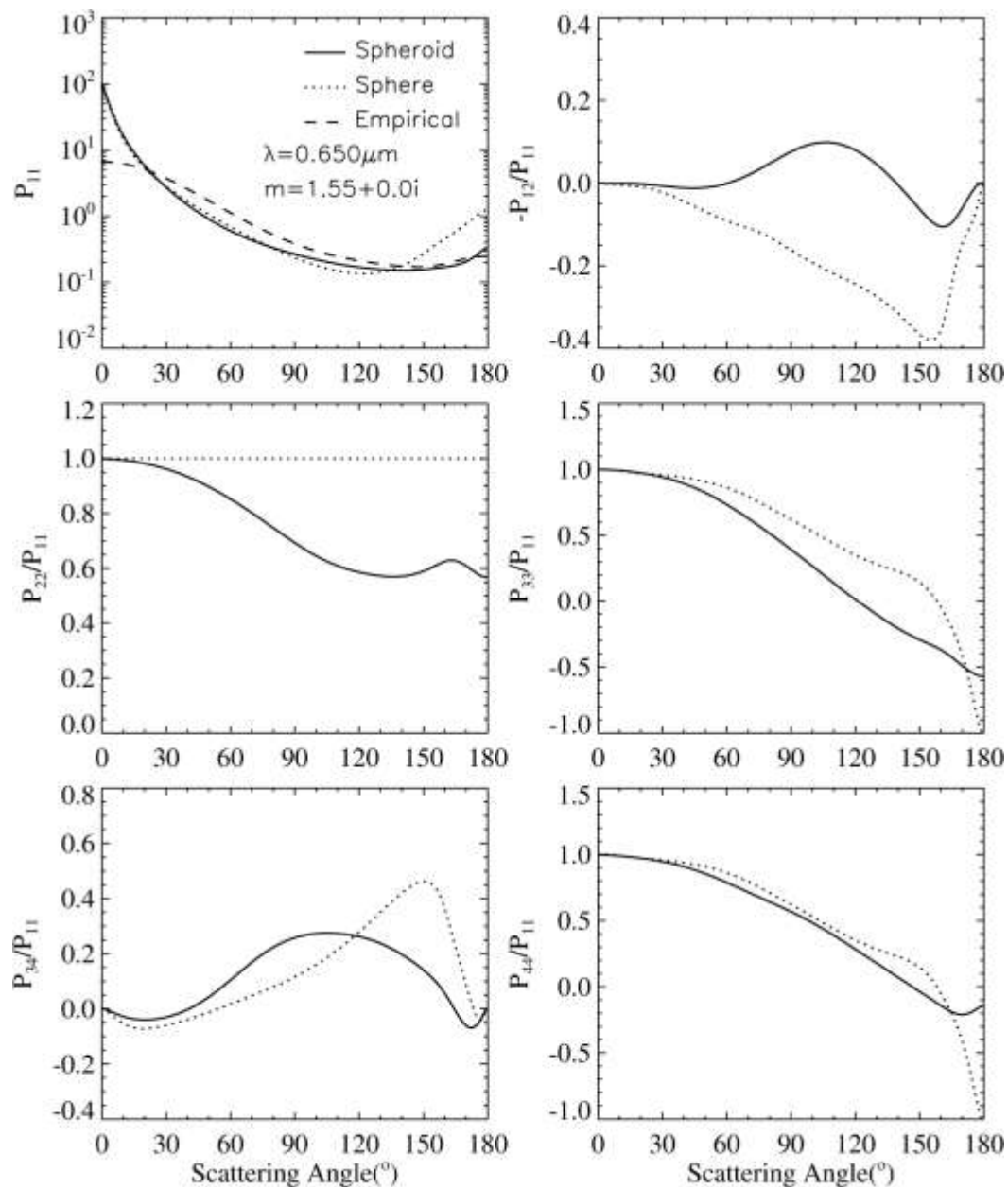




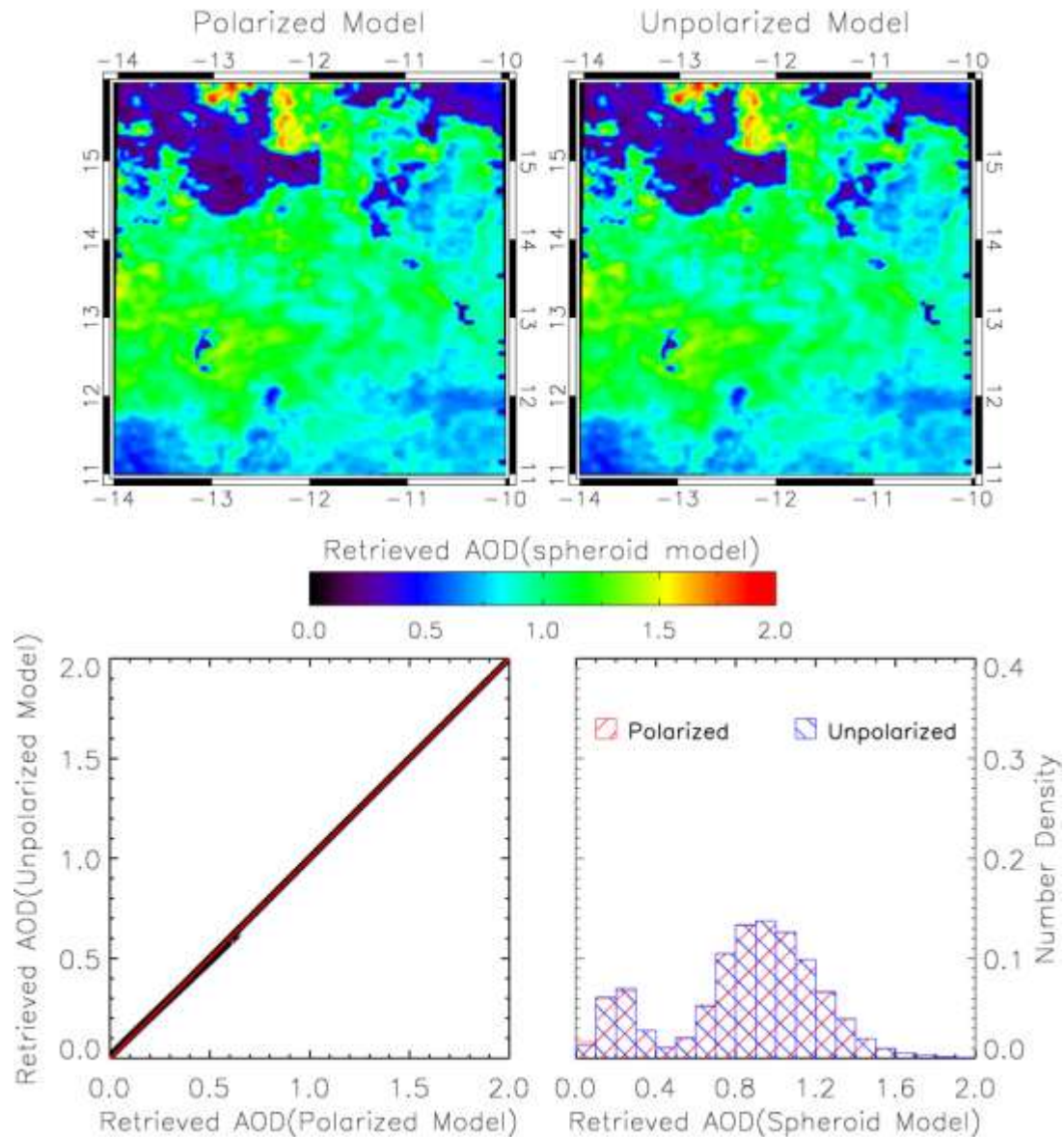
Relationship of simulated TOA upward reflectance for 0.412 versus 0.650 and 0.470 versus 0.650 as a function of aerosol optical depth and single scattering albedo. The red line and blue line correspond to spheroid model and sphere model, respectively. Different single scattering albedo corresponds to different refractive index: $(1.55+0.0i)$, $(1.55+0.001i)$, $(1.55+0.002i)$, $(1.55+0.003i)$.

Spheroid Model vs Sphere Model





Polarized Model vs Unpolarized Model



Part IV

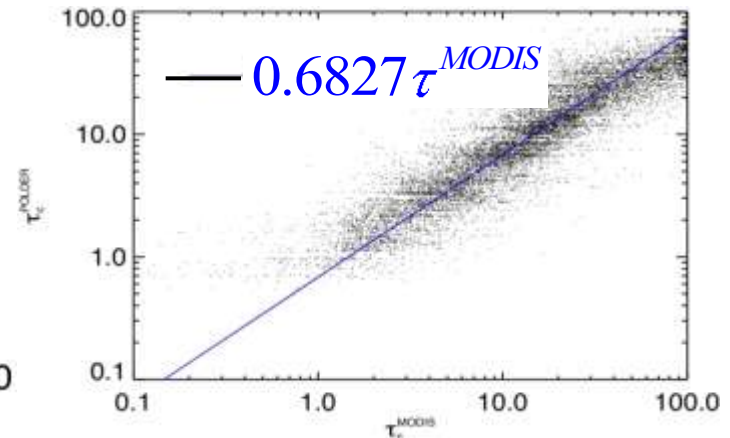
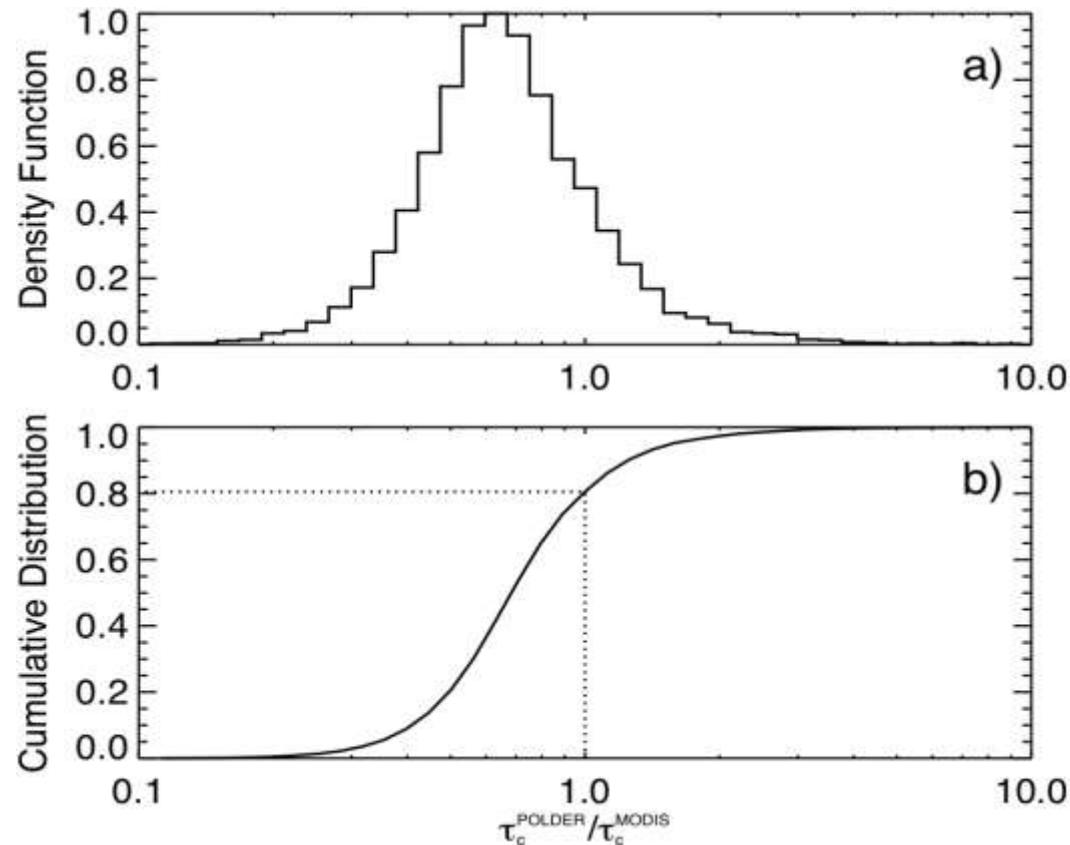
Compare MODIS and POLDER Cirrus Cloud Property Retrievals

Difference between MODIS and POLDER retrieval algorithms

	MODIS	POLDER
Resolution	1km	20km
Particle effective size	Retrieved	Assumed ¹
Bulk scattering model	Baum05 ²	IHM ³
Directionality	Single	Up to 16

1. r_e of ice clouds is assumed to be 30 μ m in POLDER retrieval
2. Baum, B. A., P. Yang, A. J. Heymsfield, S. Platnick, M. D. King, Y. X. Hu, and S. T. Bedka, 2005: Bulk Scattering Properties for the Remote Sensing of Ice Clouds. Part II: Narrowband Models. *Journal of Appl. Meteor.*, **44**, 1896-1911.
3. C.-Labonnote, L., G. Brogniez, M. Doutriaux-Boucher, J. C. Buriez, J. F. Gayet, and H. Chepfer, 2000: Modeling of light scattering in cirrus clouds with inhomogeneous hexagonal monocrystals. Comparison with in-situ and ADEOS-POLDER measurements. *Geophys. Res. Lett.*, **27**, 113-116.)

MODIS τ vs POLDER τ



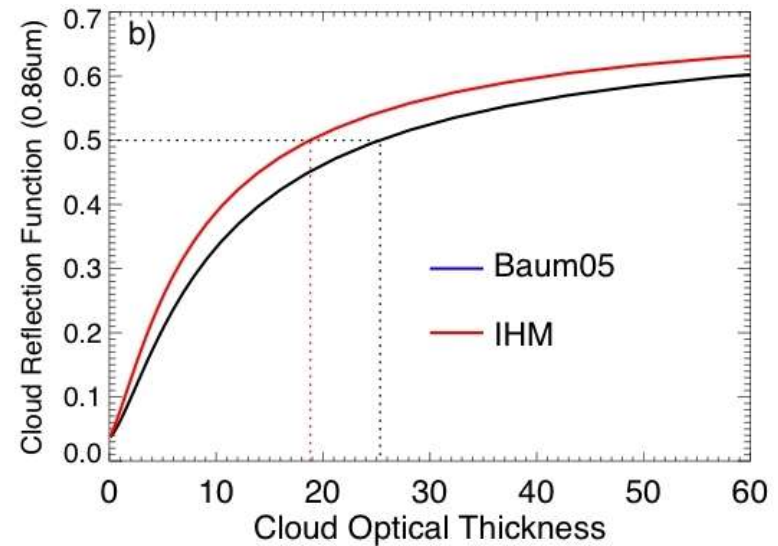
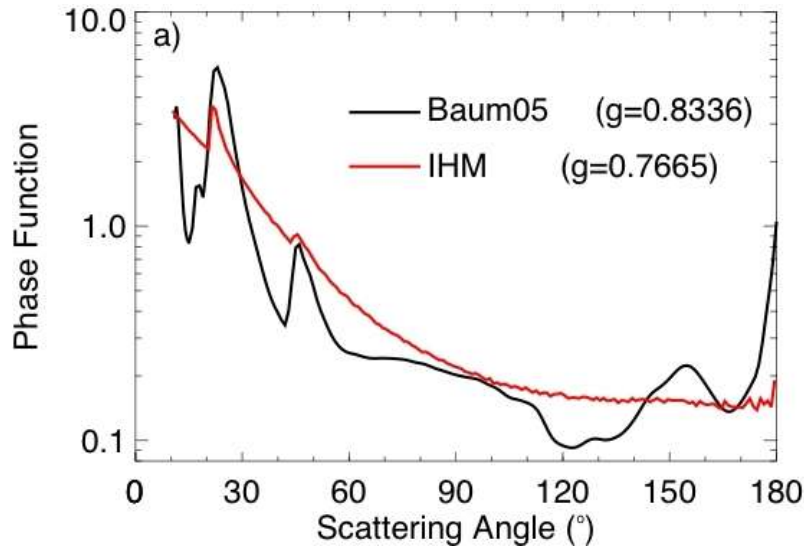
- ❖ $\tau^{POLDER} / \tau^{MODIS}$ follows the **log-normal** distribution
- ❖ τ^{POLDER} is substantially smaller than τ^{MODIS}

For more than 80% pixels
 $\tau^{POLDER} < \tau^{MODIS}$

For more than 50% pixels
 $\tau^{POLDER} < \tau^{MODIS}$ by more than 30%

Main reason for the difference

- Difference in bulk scattering model



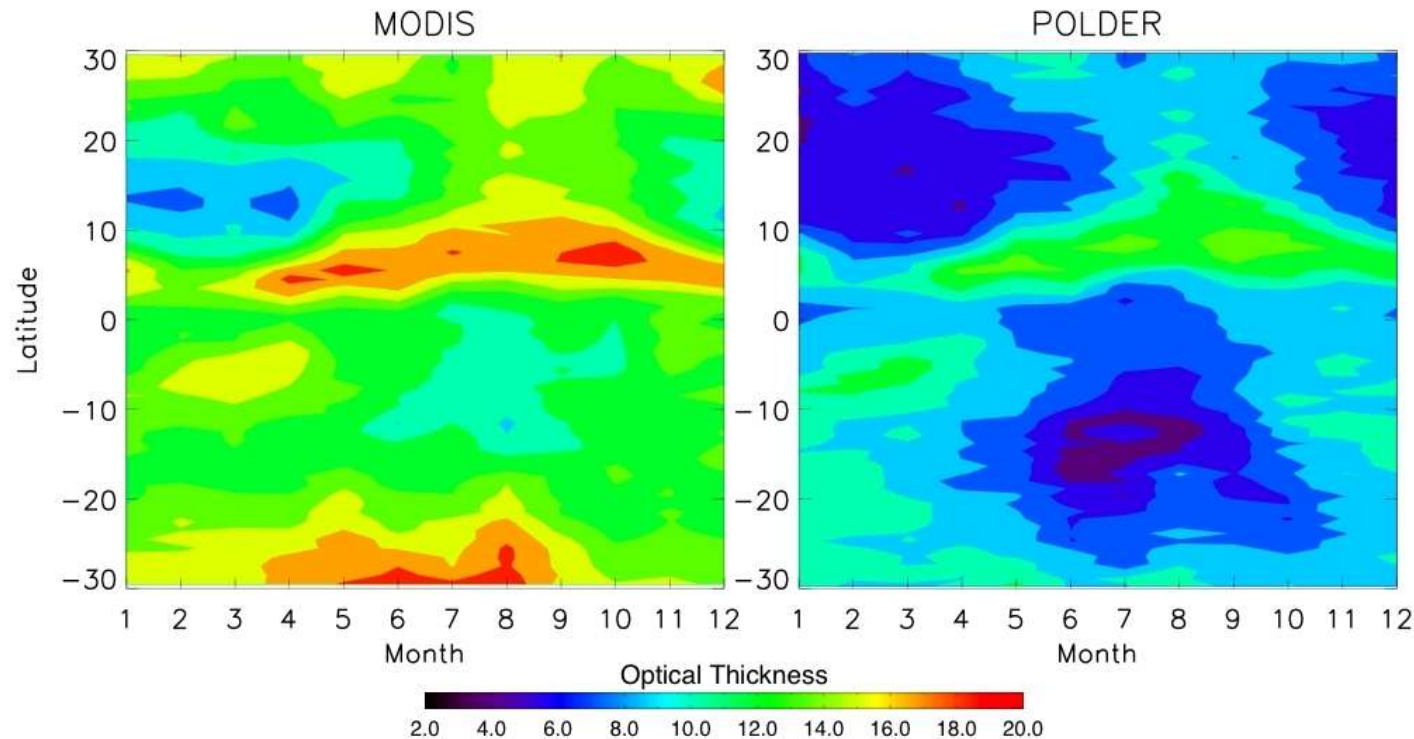
$$R \sim (1 - g)\tau$$

$$\tau^{\text{retrieval}} \sim R^{\text{obs}} / (1 - g)$$

$$\frac{\tau^{\text{POLDER}}}{\tau^{\text{MODIS}}} \sim \frac{1 - g^{\text{Baum05}}}{1 - g^{\text{IHM}}} = 0.7126 \quad (\text{From data: } 0.6827)$$

Implications for cirrus SW CRF

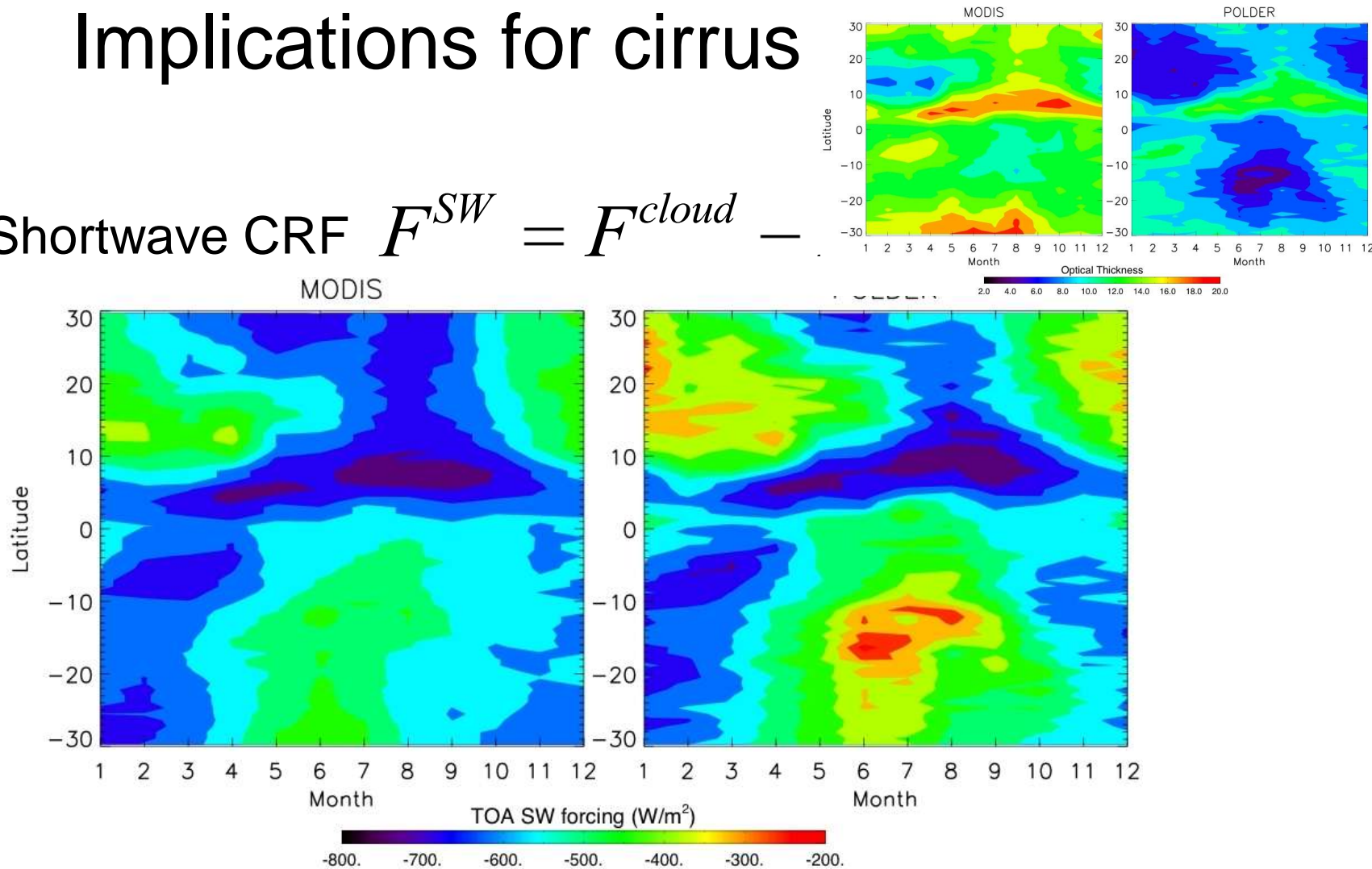
Zonal mean cirrus optical thickness vs month (2006)



Annual area-averaged $\tau^{\text{POLDER}} < \tau^{\text{MODIS}}$ by about 40%

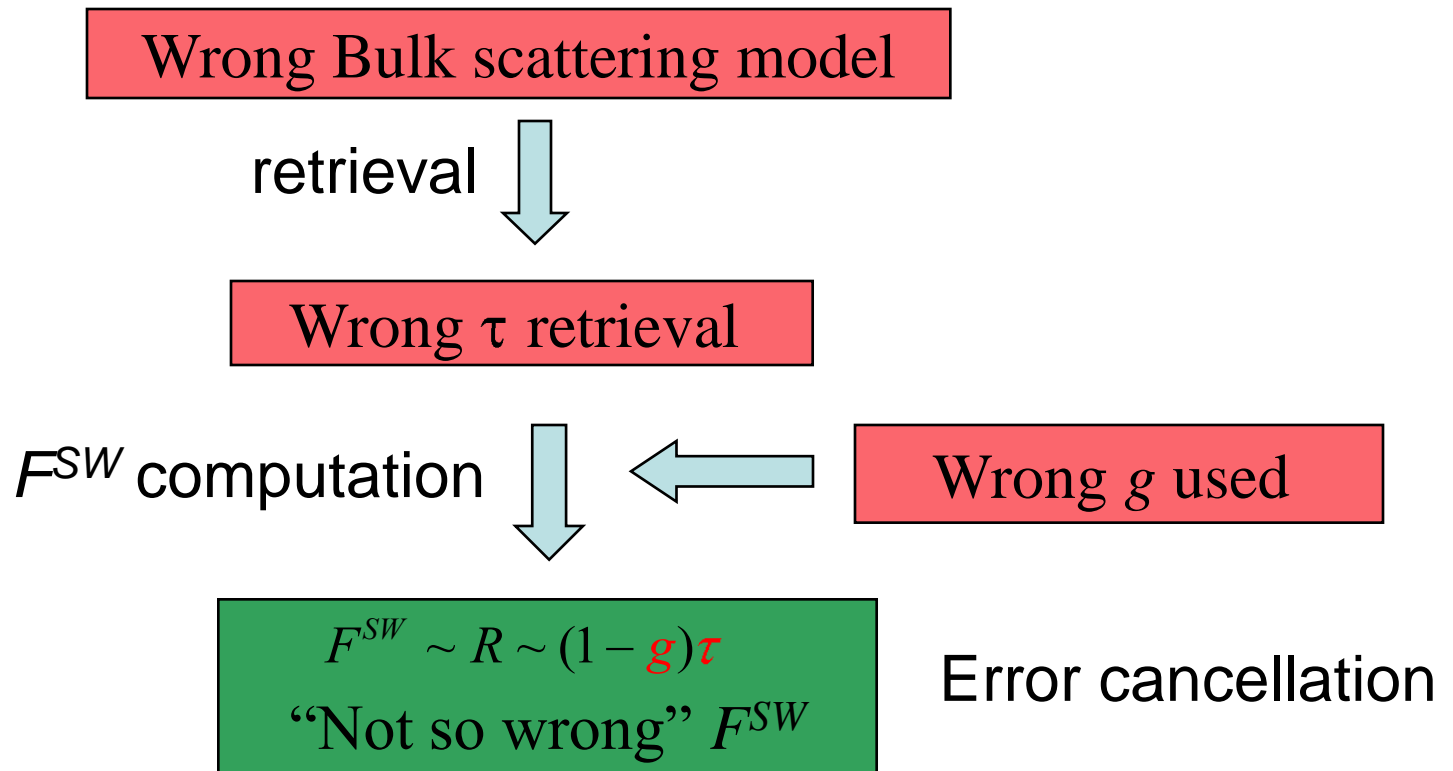
Implications for cirrus

Shortwave CRF $F^{SW} = F^{cloud}$ —



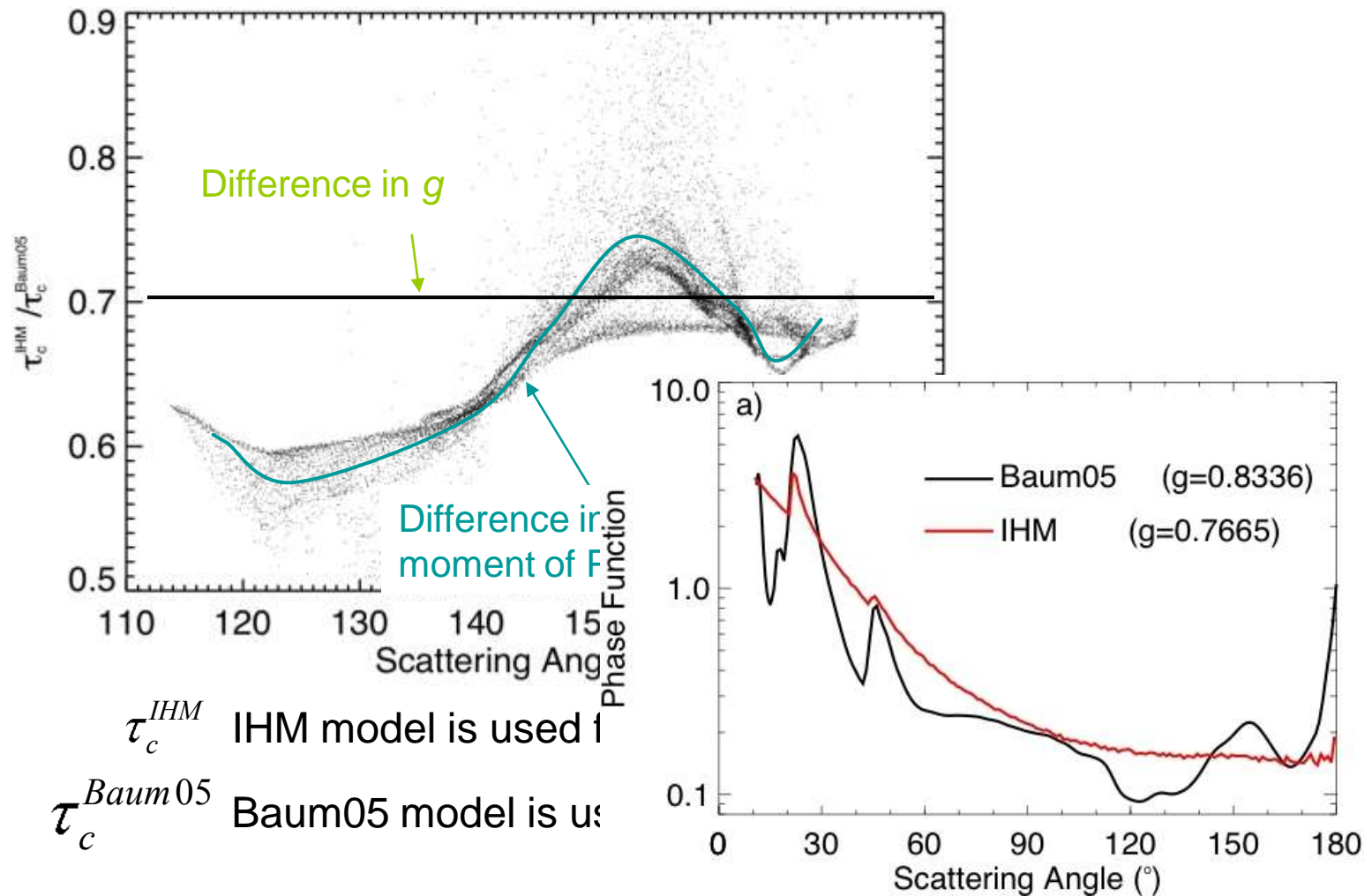
Difference in annual area-averaged F^{SW} is within 10%

Implications for cirrus SW CRF



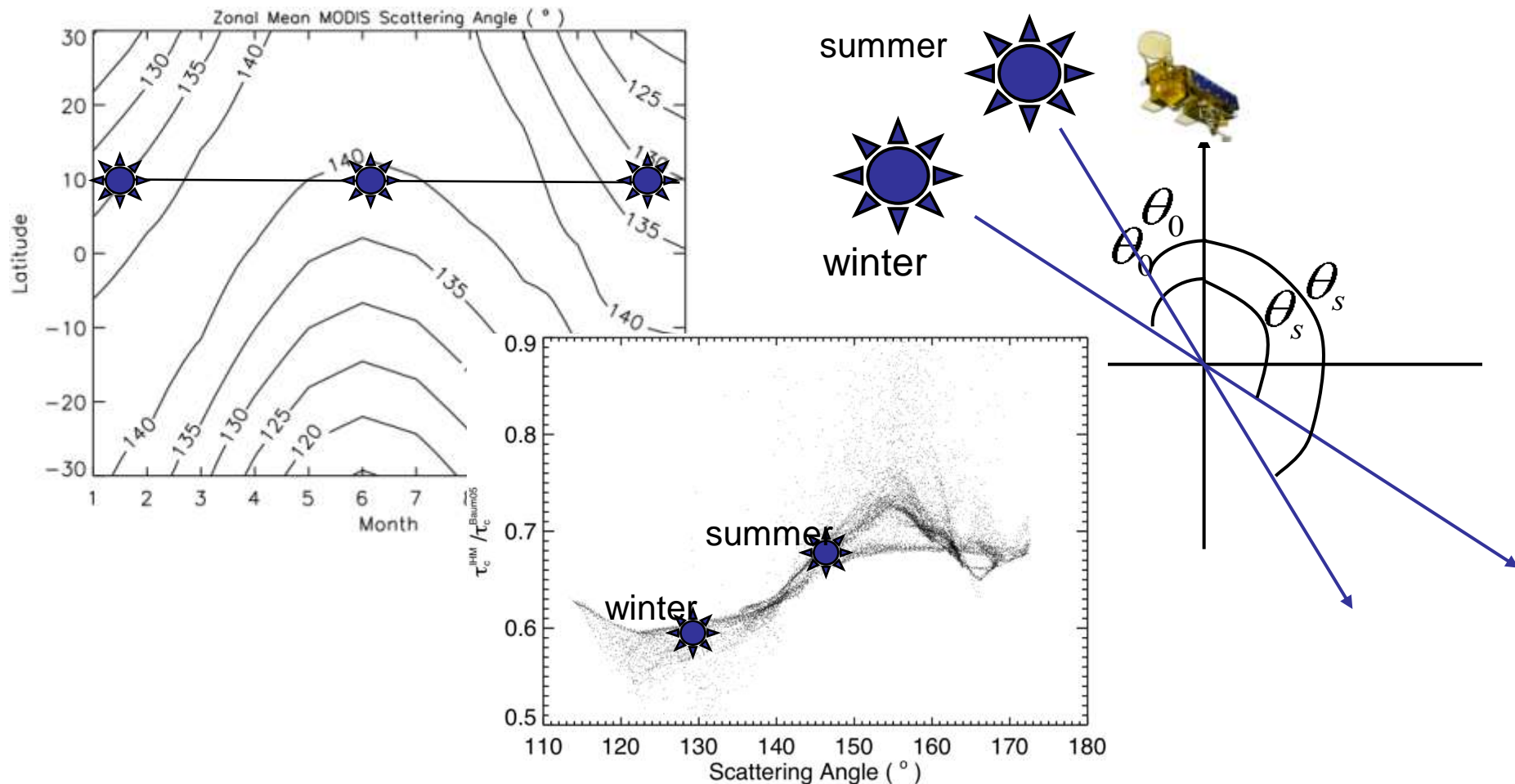
Does the bulk scattering model really matter?
Yes, see the following example.

Bulk scattering model and seasonal variation of τ retrieval

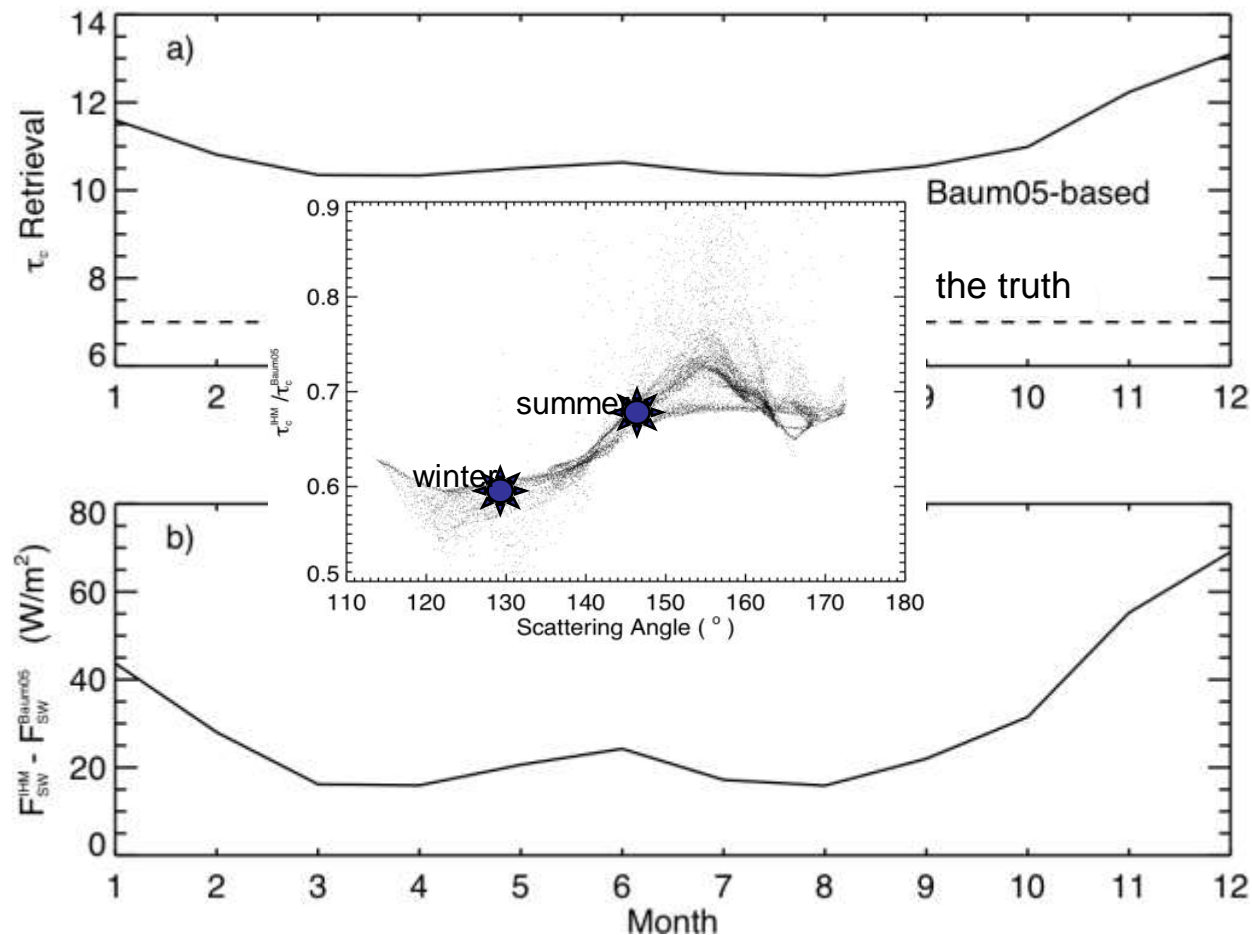


Bulk scattering model and seasonal variation of τ retrieval

MODIS angular sampling vs season



Bulk scattering model and seasonal variation of τ retrieval



Summary

These studies are still on-going efforts.

We will report our progress at the next MODIS/VIIRS meeting.